

AMR Seminar #69

Case – 1

Contributed by: Abbas Agaimy

Clinical history: A 62-year-old man presented with leukocytosis (13.000), thrombocytopenia (5.000) and macrocytic anemia (hemoglobin 10.7 mg/dl). Bone marrow trephine biopsy showed reactive hypercellular marrow. Upper GI endoscopy was negative for neoplasia. Colonoscopy revealed two small low-grade tubular adenomas. Imaging revealed a huge right adrenal mass and a 1 cm nodule in the gastric wall. Clinical suspicion diagnosis was either adrenocortical carcinoma or pheochromocytoma. Serology was negative for catecholamines. He underwent right adrenalectomy and wedge excision of the gastric lesion.

Microscopic Features: The adrenalectomy specimen was completely occupied by a mass of 15.5 x 11 x 10 cm size with extensively necrotic brown to tan cut-surface and friable soft consistency.

Histological & Immunohistochemical findings: Histologically, the adrenal tumor was composed of diffuse poorly cohesive sheets of medium-sized to large relatively monomorphic epithelioid cells with vascular nuclei and prominent centrally located nucleoli. Focal rhabdoid cell features were noted. The background stroma showed mixed inflammatory cell infiltrates and a few residual adrenal cortical cell aggregates in-between. There was no specific differentiation features or secretory activity. All 14 sampled lymph nodes within adjacent retroperitoneal fat were free of tumor.

Immunohistochemistry showed diffuse expression of pancytokeratin (AE2/AE3; Fig.A) and vimentin. HepPar-1 was strongly and diffuse positive with distinctive coarse granular cytoplasmic pattern (Fig. B). Polyclonal CEA showed very focal canalicular staining (Fig. C). All other markers were negative (calretinin, inhibin, Melan A, synaptophysin, chromogranin A, Glypican3, Arginase-1, AFP, TTF1, CDX2, HMB45, CD56, MDM2, CDK4, protein S100, desmin, ERG, CD31). The SWI/SNF proteins SMARCB1, SMARCA4 and ARID1A were intact in the tumor cells. Melan A highlighted residual adrenal cortical tissue at the periphery (Fig. D). We still have no well functioning SF-1 antibody. The gastric wall nodule turned out to be a small spindle cell benign GIST (0 risk according to Miettinen & Lasota system).

Diagnosis: Poorly differentiated carcinoma with hepatoid differentiation. Further workup to exclude HCC and other HepPar-1 positive (e.g. lung) carcinoma was recommended and was negative including liver CT, sonography and MRI. Primary hepatoid adrenal carcinoma was favored as a diagnosis by exclusion.

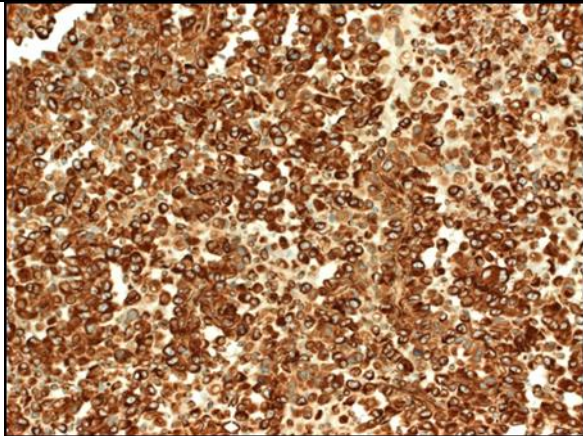
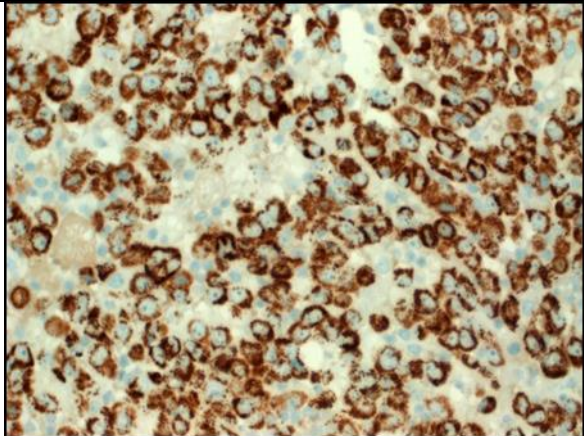
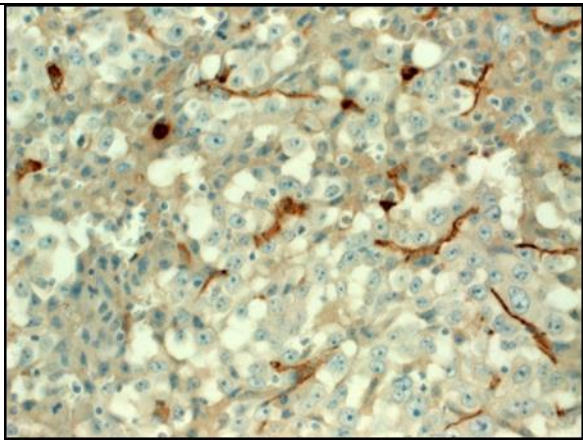
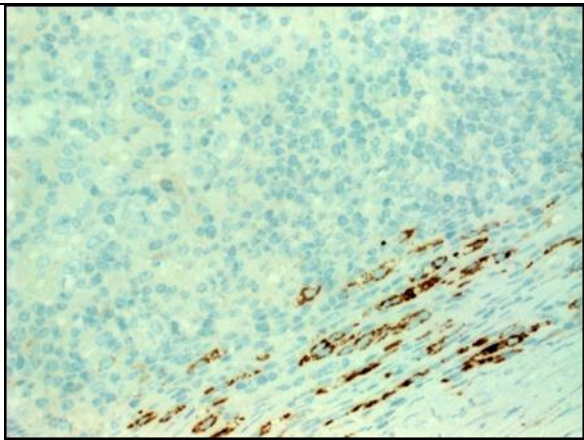
Comment: Metastatic adrenal tumors are much more common than primary adrenocortical carcinoma. NSCLC is the major source of adrenal gland metastasis. Accordingly, diagnosis of primary adrenocortical carcinoma relies not only on well-established characteristic features, but also on exclusion criteria to rule out metastatic disease. The case presented herein is unusual due to two reasons:

1. Adrenal metastasis from occult HCC is documented as a quite rare and misleading presentation of hepatic HCC being reported in isolated case reports.
2. Hepatoid carcinoma can closely mimic adrenocortical carcinoma, both histologically and clinically/on imaging.

These two factors complicate the differential diagnostic workup of such a case. The abundance of cytokeratins is essentially considered a potential clue to a non-adrenal origin as primary adrenocortical neoplasms are frequently cytokeratin-poor, but this feature is not reliable to exclude primary adrenocortical carcinoma. In this particular case, discussion of the findings with the clinicians and careful examination of the liver uncovered a history of alcohol abuse and presence of minute liver nodules interpreted as hemangiomas on imaging. Thus, it is very likely that this case represents genuine hepatoid primary adrenocortical carcinoma. Given that the incidence of synchronous metastasis at the time of HCC diagnosis is high (37%) with adrenal metastasis comprising 11% in one series, primary hepatoid adrenocortical carcinoma should be a diagnosis of exclusion. To date, less than 5 cases of occult HCC presenting with huge (>10 cm) adrenal metastases closely mimicking a primary adrenal malignancy have been reported [1-3].

The most widely used IHC markers for hepatocellular differentiation are HepPar-1, Arginase-1, Glypican-3, CD10, polyclonal CEA and others recently reported markers. However, none is specific for HCC or hepatoid differentiation. Hep-Par-1 is expressed in subsets of adenocarcinomas of upper GI tract, pancreatobiliary system, urinary tract and in particular in a subset of NSCLC [4-6], although many of these cases do not reveal unequivocal hepatoid features on HE stain [7-10]. Based on this, and given the well-known tendency of NSCLC to metastasize to the adrenal, it is mandatory to rule out a lung primary which is ruled out in this case by negative imaging and clinical examination. Distinguishing HCC metastasis from HePPar-1-positive carcinomas might be difficult or on occasion even impossible by histology alone. However, a valuable clue to hepatoid carcinoma vs. HCC is the very frequent expression of CK7 in the former and its almost uniform absence in true HCC. Arginase-1 has emerged as more sensitive and more specific marker for HCC [11,12]. Although in my experience (unpublished data) and from the literature, Arginase-1 is usually negative in Hep-Par1+ carcinomas other than HCC, a very recent study showed its detection in 5 of 8 hepatoid carcinomas from different organs [13]. However, hepatoid carcinomas of the adrenal seem to be very rare (or under-recognized) with very few putative cases reported [14]. The most important consideration in the current case is rhabdoid adrenocortical carcinoma, three examples of which have been recently reported by Saul in Histopathology [15]. The current case showed focal rhabdoid cell features. The Saul´s series showed consistent immunoprofile similar to conventional adrenocortical carcinoma. Thus the current case seems not to fit the rhabdoid variant of adrenocortical carcinoma. Also, epithelioid angiosarcoma of the adrenal (one such case presented in a previous AMR series by Markku) may occasionally show rhabdoid features and express pancytokeratin, thus being a possibility to be ruled out by negative endothelial markers or presence of clear-cut vasoformation.

I would be glad to hear the experience of the Club members with this unusual neoplasm/presentation.

<div data-bbox="203 915 334 940">A: AE1/AE3</div> 	<div data-bbox="823 915 961 940">B: HepPar-1</div> 
<div data-bbox="203 1379 280 1404">C: CEA</div> 	<div data-bbox="823 1379 945 1404">D: Melan-A</div> 

REFERENCES

1. Tsalis K, Zacharakis E, Sapidis N, et al. Adrenal metastasis as first presentation of hepatocellular carcinoma. *World J Surg Oncol*. 2005; 3: 50.
2. Mundada P, Tan ML, Soh AW. Radiologically occult hepatocellular carcinoma in a cirrhotic liver presenting with bilateral adrenal metastases. *Med J Malaysia*. 2015 Aug;70(4):256-8.
3. Bhosale P, Szklaruk J, Silverman PM. Current staging of hepatocellular carcinoma: imaging implications. *Cancer Imaging*. 2006; 6:83-94.
4. Wennerberg AE, Nalesnik MA, Coleman WB. Hepatocyte paraffin 1: a monoclonal antibody that reacts with hepatocytes and can be used for differential diagnosis of hepatic tumors. *Am J Pathol* 1993;143:1050-4.
5. Lamps LW, Folpe AL. The diagnostic value of hepatocyte paraffin antibody 1 in differentiating hepatocellular neoplasms from nonhepatic tumors: a review. *Adv Anat Pathol* 2003;10:39-43.
6. Lugli A, Tornillo L, Mirlacher M, Bundi M, Sauter G, Terracciano LM. Hepatocyte paraffin 1 expression in human normal and neoplastic tissues: tissue microarray analysis on 3,940 tissue samples. *Am J Clin Pathol* 2004;122:721-7.
7. Mac MT, Chung F, Lin F, Hui P, Balzer BL, Wang HL. Expression of hepatocyte antigen in small intestinal epithelium and adenocarcinoma. *Am J Clin Pathol* 2009;132:80-5.
8. Yousem SA, Lale S, Dacic S. HepPar-1 expression in primary lung adenocarcinoma. *Am J Clin Pathol* 2013;140:225-30.
9. Haninger DM, Kloecker GH, Bousamra Ii M, Nowacki MR, Slone SP. Hepatoid adenocarcinoma of the lung: report of five cases and review of the literature. *Mod Pathol* 2014;27:535-42.
10. Giedl J, Büttner-Herold M, Wach S, Wullich B, Hartmann A, Agaimy A. Hepatocyte Differentiation Markers in Adenocarcinoma of the Prostate: HepPar-1 but not Arginase-1 is specifically expressed in a Subset of Prostatic Adenocarcinoma. *Hum Pathol*, 2016 Epub.
11. Yan BC, Gong C, Song J, et al. Arginase-1: a new immunohistochemical marker of hepatocytes and hepatocellular neoplasms. *Am J Surg Pathol* 2010;34:1147-54.
12. Sang W, Zhang W, Cui W, Li X, Abulajiang G, Li Q. Arginase-1 is a more sensitive marker than HepPar-1 and AFP in differential diagnosis of hepatocellular carcinoma from nonhepatocellular carcinoma. *Tumour Biol* 2015;36:3881-6.
13. Chandan VS, Shah SS, Torbenson MS, Wu TT. Arginase-1 Is Frequently Positive in Hepatoid Adenocarcinomas. *Hum Pathol*. 2016 Epub.
14. Malya FU, Bozkurt S, Hasbahceci M, Cipe G, Ahmad IC, Gucin Z, Karatepe O, Muslumanoglu M. A rare tumor in a patient with hepatic hydatid cyst: adrenal hepatoid adenocarcinoma. *Case Rep Med*. 2014;2014:824574.
15. Weissferdt A, Phan A, Suster S, Moran CA. Primary rhabdoid adrenocortical carcinoma: a clinicopathological and immunohistochemical study of three cases. Primary rhabdoid adrenocortical carcinoma: a clinicopathological and immunohistochemical study of three cases. *Histopathology*. 2013;62:771-7.

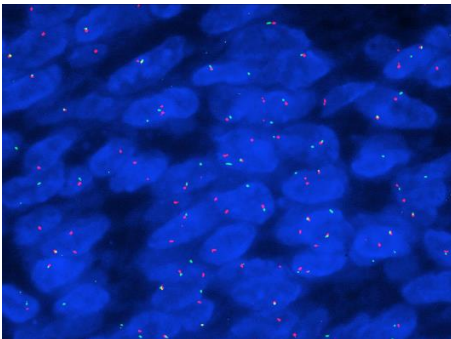
AMR Seminar #69

Case – 2

Contributed by: Gerald Berry, M.D.

Clinical History: A 44-year old man underwent surgical exploration in February 2016 at another institution to relieve cardiac tamponade. A mass was discovered in the posterior pericardium measuring 8x6x4 cm. It was resected and sent to the surgical path lab.

Pathology Findings: Sections display a malignant spindle cell neoplasm arranged in a vague fascicular pattern along with scattered gaping vessels. The neoplastic cells exhibit scant cytoplasm, hyperchromatic nuclei with minimal cytoplasm. Focally, some of the cells display clear to pale cytoplasm. Division figures are numerous but pleomorphism and necrosis are minimal or absent. Along with the H&E stained slides came a battery of immunostains that were all negative: CK5/6, WT1, CDK4, MDM2, calretinin, D2-40, SMM, CD40, EMA, CAM 5.2, S100, actin, desmin, and Sox-10 with only vimentin staining observed. The proliferation rate was high. MDM2 had been performed elsewhere and was negative. I added 1 immunostain, Stat 6 to exclude a malignant SFT and sent off for *SYT* gene rearrangement (see attached image).



Diagnosis: Monophasic synovial sarcoma of the pericardium

Comment: I wanted to submit this case primarily for its rarity in this location. A perusal of the literature yields mostly case reports with attendant literature reviews. There appears to be less than 20 cases published in the English literature. Most cases arise in younger folks (<40 years) with a slight predilection for males. Clinical signs and symptoms relate to local compressive issues such as tamponade: chest pain, dyspnea, cough although systemic symptoms like fever and fatigue have been reported. Invasion of adjacent mediastinal structures at the time of diagnosis is not uncommon. The lesions, as in this case, tend to be large at the time of diagnosis (6-15 cm). The biphasic SS pattern is slightly more common than monophasic SS in the study by Cheng et al.

The differential diagnostic considerations after metastasis include sarcomatoid or biphasic malignant mesothelioma, sarcomatoid carcinoma, malignant SFT, and other sarcomas. Immunostaining can be helpful to exclude malignant

mesothelioma although they tend to arise in much older patients. Fluorescence in situ hybridization is most helpful in establishing the diagnosis by demonstrating rearrangement of the *SYT* gene.

The prognosis is extremely poor both given the type of neoplasm, the presence of invasion of local structures at the time of diagnosis and the high rate of local recurrence/distant metastasis. Surgical resection/debulking followed by chemotherapy are the main treatment options. Multi-agent chemotherapy regimens include dacarbazine and ifosfamide +/- radiation therapy. Survival rates that are reported range from 20-50% at 5 years but this is quite optimistic.

References: Anand AK, Khanna A, Sinha SK et al. Pericardial synovial sarcoma. Clin Oncol 2003; 15:186-188.

Cheng Y, Sheng W, Zhou X, et al. Pericardial synovial sarcoma, a potential for misdiagnosis: clinicopathologic and molecular cytogenetic analysis of 3 cases with literature review. Am J Clin Pathol 2012; 137:142-149.

Muramatsu T, Takwshita S, Tanaka Y, et al. Primary pericardial synovial sarcoma. J Thorac Dis 2015; 7:E496-E498.

AMR Seminar #69

Case – 3

Contributed by: Thomas V. Colby, M.D.

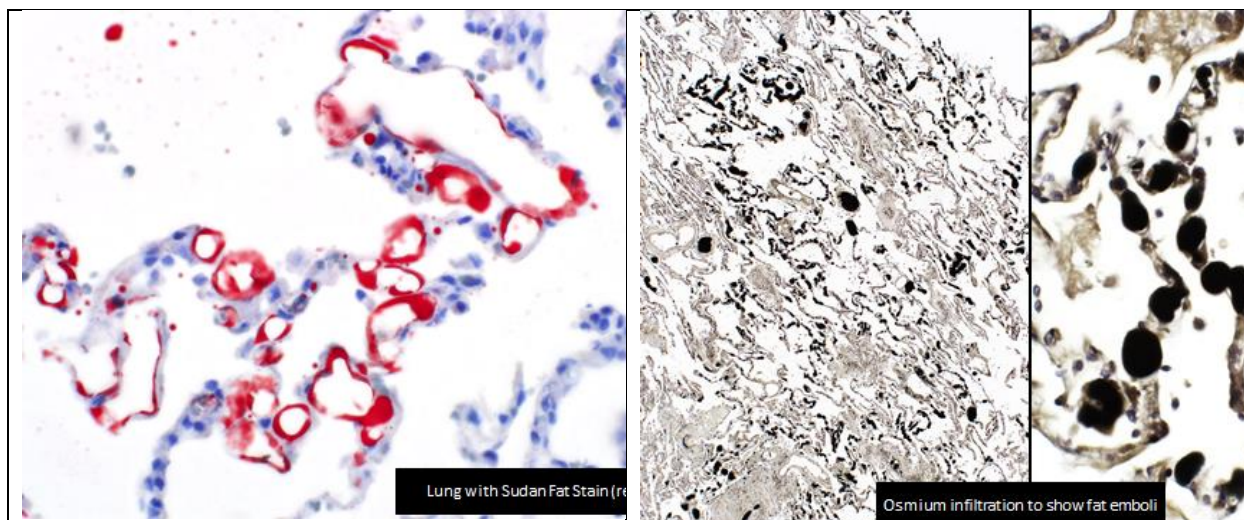
Case History: A 58-year-old man with end-stage liver disease secondary to alcohol abuse and end-stage renal disease secondary to hepato-renal syndrome was brought to the OR for a combined deceased donor liver-kidney transplantation. The liver allograft was prepared and implanted first. It was an allograft that was grossly acceptable to the surgeon; some grossly evident fatty change was noted but not out of the ordinary. There was good vascular flow and anastomoses. The renal allograft was then implanted. Just before reperfusion of the kidney, there was a sudden loss of blood pressure despite adequate cardiac status and no evident bleeding. The patient continued to deteriorate and to show oxygen desaturation and to have frothy output from his anesthesia tube. The patient was transferred to the ICU with vasodilatory shock and progressive hypoxemia. There was no significant bony trauma.

Upon arrival in the ICU, the patient had profoundly low systemic vascular resistance, and despite all available aggressive measures, he progressively deteriorated and died approximately five hours after transfer to the ICU. Clinical diagnoses were:

1. Severe refractory vasodilatory shock likely related to septic shock and inflammatory mediator cytokines from the liver allograft.
2. Severe ARDS.
3. Severe metabolic and respiratory acidosis, unresponsive to treatment.
4. Chronic renal failure.
5. End-stage liver disease.
6. Progressive coagulopathy in the setting of shock despite early corrective measures.

Autopsy was performed. The heart was 420 grams without significant abnormalities and no evidence of infarct. The combined weight of the lungs was 1670 grams. Pleural surfaces were smooth and glistening. Cut sections show congestion and exuded bloody serous fluid. No thrombo-emboli were identified. The allograft liver was red-brown and soft on cut section. The capsule was intact. All the vascular anastomoses were intact without leakage.

Microscopic sections of the liver show centrilobular hemorrhagic necrosis with clear spaces consistent with fat from necrotic liver cells. On careful inspection, one can find some cellular debris in terminal hepatic venules. Sections of the lung show numerous fat emboli confirmed with Sudan fat stains of frozen sections of formalin fixed tissue and osmium infiltration (see below). The osmium process is as follows: take a small piece of formalin fixed tissue and infiltrate with osmium as you would for EM and then process for routine H&E. Both fat stains are shown below.



Discussion: Despite the relatively high frequency of allograft livers showing some degree of fatty change at the time of implantation, fat emboli from the allograft is almost unheard of and only one case could be found in a series from UC San Francisco (below). Slides from that case were reviewed and showed identical features to the current case (courtesy Kirk Jones, M.D.).

In the series from UC San Francisco, there were eight patients who developed rapid respiratory failure immediately following liver allograft implantation. Seven of those had TRALI (transfusion-related acute lung injury), and all of those patients survived. One had fat emboli, and that patient died intraoperatively and autopsy showed features identical to the case presented.

I present this as an interesting and unusual example.

Reference: Yost CS et al. Etiology of acute pulmonary edema during liver transplantation. A series of cases with analysis of the edema fluid. Chest. 2001; 119:219.

AMR Seminar #69

Case – 4

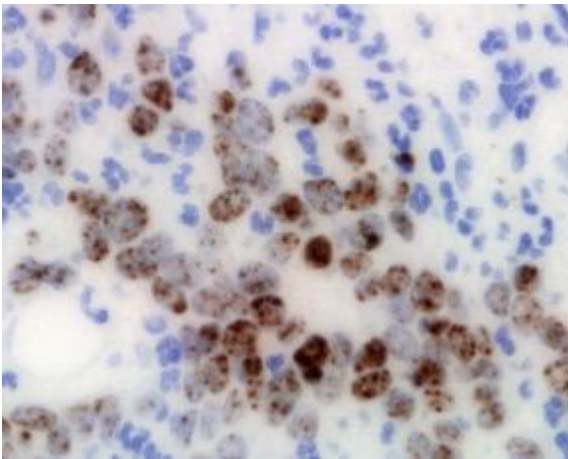
Contributed by: Cyril Fisher, M.D.

Clinical History: A 39 year old female had an infiltrative tumor of the parotid gland.

Pathologic Features: The tumor is disposed in cords and nests of undifferentiated but relatively uniform small to medium-sized polygonal cells in acutely inflamed stroma. There are also islands of better-differentiated squamous cells. Immunohistochemistry showed focal positivity for CK, EMA, and p63 and focal CD34. INI1 was retained (positive in nuclei) and NUT was focally positive (image provided). EBER and p16 were negative. FISH revealed *BRD4* gene rearrangement (this was kindly carried out by Dr Chris French in Boston who has authored many of the reports on this tumor type).

Diagnosis NUT midline carcinoma of salivary gland.

Comment: NUT carcinoma was first identified in 1991 (Kubonishi et al) as a variant of thymic carcinoma presenting as a very aggressive midline mediastinal tumor. It has now been described in other locations especially head and neck sites (accounting for about a third of cases), including, rarely, (and not in the midline) in parotid gland, (e.g. den Bakker et al [2009], who also described chondroid differentiation), pancreas, bladder, and lung. It can occur at any age but appears to be more frequent in younger patients. It is a poorly differentiated squamous cell carcinoma with demarcated islands of better-differentiated SCC. The stroma is usually fibrous and inflammation as seen here is not a usual feature, though necrosis is common.



The tumor cells can coexpress CK, p63 and CD34, which is a useful clue as CD34 is rarely found in carcinomas. The INI1 positivity helps to exclude epithelioid sarcoma. Nuclear positivity with antibody to NUT, in a typical speckled pattern, is diagnostic. This relates to the underlying t(15;19)(q13;p13.1) with rearrangement of *NUT* (NUclear protein in Testis) gene which fuses most commonly with *BRD4* gene, though other partners including *BRD3* have been described. The antibody is 100% specific and 87% sensitive, so that molecular confirmation is not usually needed.

Since it resembles any other SCC, this variant is likely to be more common than the literature suggests, but it is important to think of the diagnosis because of its aggressive behavior and for potential treatment. In this case the tumor metastasized to lymph node, lung and bone. Although there is no specific therapy, it has been suggested that new BET (bromodomain and extra terminal) or HAD (histone deacetylase) inhibitors might be of therapeutic use.

References

Kubonishi I, Takehara N, Iwata J, et al. Novel t(15;19)(q15;p13) chromosome abnormality in a thymic carcinoma. *Cancer Res.* 1991;51:3327–3328.

French CA, Kutok JL, Faquin WC et al. Midline carcinoma of children and young adults with NUT rearrangement. *J Clin Oncol.* 2004;22:4135-4139.

den Bakker MA, Beverloo BH, van den Heuvel-Eibrink MM, et al. NUT midline carcinoma of the parotid gland with mesenchymal differentiation. *Am J Surg Pathol.* 2009;33:1253-1258.

Bauer DE, Mitchell CM, Strait KM et al. Clinicopathologic features and long-term outcomes of NUT midline carcinoma. *Clin Cancer Res.* 2012;18:5773-5779.

French C. NUT midline carcinoma. *Nat Rev Cancer.* 2014;14:149-150.

French CA. The importance of diagnosing NUT midline carcinoma. *Head Neck Pathol.* 2013;7:11-16.

AMR Seminar #69

Case – 5

Contributed by: Andrew Folpe, M.D.

Case History: A 51-year-old man presented with chest pain. A CT scan was performed, which showed several left sided pleural based masses. Owing to clinical suspicion of malignancy, an open biopsy was performed.

Pathologic Findings: A single well-circumscribed, approximately 3cm mass was received for evaluation. Sections showed the lesion to have a thick fibrous capsule, within which were found normally organized splenic red pulp, white pulp, and pencillar arterioles.

Diagnosis: Thoracic splenosis.

Clinical Follow-up: Subsequent clinical investigation revealed that the patient had suffered a gunshot wound several years previously, with laceration of the spleen and damage to the diaphragm.

Discussion: This is a morphologically simple diagnosis, but an unusual clinical presentation- I hope the AMR slide club members will forgive me for submitting such a pedestrian case!

Thoracic splenosis is a rare but well-recognized complication of thoraco-abdominal trauma, with fewer than 40 cases in the English language literature, chiefly in the form of case reports in surgical journals. The interval between the initial trauma and discovery of thoracic splenosis averages 16 years. There is some evidence of suggest that splenosis is protective against sepsis in otherwise asplenic patients, and thus removal of ectopic splenic tissue is contraindicated. Pre-operative diagnosis can be suggested by CT and radionuclide imaging studies, if a clinical history of prior splenic and diaphragmatic injury is known. The differential diagnosis includes ectopic spleen (intra-abdominal, no history of trauma) and anastomosing hemangioma of soft tissue, a rare lesion that may somewhat simulate splenic tissue, but which lacks true red and white pulp or pencillar arterioles.

References:

Bibliography

1. O'Connor JV, Brown CC, Thomas JK, et al. Thoracic splenosis. *Ann Thorac Surg.* 1998;66:552-553.
2. John I, Folpe AL. Anastomosing Hemangiomas Arising in Unusual Locations: A Clinicopathologic Study of 17 Soft Tissue Cases Showing a Predilection for the Paraspinal Region. *Am J Surg Pathol.* 2016. (epub available online)

AMR Seminar #69

Case – 6

Contributed by: Ondřej Hes, M.D., Ph.D.

Case History: 71-year-old Caucasian male was admitted to the hospital because of macroscopic hematuria. Cystoscopy revealed a large pedunculated mass in the apical part of the urinary bladder, more than 5 cm in largest diameter. Endoscopic biopsy was taken and based on the results a radical cystectomy was performed.

Gross Pathology: Specimen was 16.5 x 10.5 x 3 cm, with attached prostate 3.5 x 3 x up to 2 cm. Urinary bladder was 7.5 x 5 x up to 3 cm with wall 1.4 cm thick. In the apical portion there was a tumor 5.4 x 3.5 x 2 cm, hemorrhagic and necrotic with invasive growth into the wall of bladder and into perivesical lipomatous tissues.





Histology: Bladder: Areas of an invasive, lymphocyte-rich mass were found in the bladder apex. The tumor was largely necrotic and hemorrhagic and composed of discohesive high grade cells with eccentric large polymorphous nuclei, prominent nucleoli, voluminous cytoplasm and edematous loose stroma. Cytoplasm was mostly weakly eosinophilic. Typical urothelial carcinoma component was not documented.

Neoplastic cells were positive for CK 7, OSCAR and focally with CD56. Negative reaction was documented with CK 20, PSA, PAPH, CD45, CD3, CD5, CD20, CD79a and melanocytic markers (HMB45, S100, Melan A).

Angioinvasion and invasion into the fatty tissues were encountered. Peritoneal surface was intact. Several metastases were found in lymph nodes.

In the prostate, which was submitted as whole mount specimen, pT2c prostatic acinar adenocarcinoma, Gleason score 6 (3+3) was found. Urothelial tumor was not present within the prostatic stroma.

Diagnosis: Plasmacytoid urothelial carcinoma (PUC).

Comments: Most PUCs are discovered in high stage with deep invasion of the bladder wall and perivesical tissue. Usually high risk for peritoneal involvement is mentioned. Our case was diagnosed in high stage (invasive tumor with metastases in lymph node).

Tumor is typically composed of cells resembling plasma cells located in loose or myxoid, usually edematous stroma. Cells grow in nests or sheets; however, they frequently tend to infiltrate the stroma as single cells. Cells show abundant eosinophilic (rarely basophilic) cytoplasm and eccentric nuclei. Retraction artifacts are common. Several authors described such morphology as lymphoma-like or lobular breast carcinoma-like.

PUC were described in association with signet ring-like component. Sometimes, PUCs produce edematous lesion, resembling bladder wall inflammation, inconspicuous thickening rather than polypoid mass. According to some

authors, edema is an important feature. In bladder biopsy or TUR with clinical impression of tumor, a presence of mucosal edema should raise the question of possible diagnosis of PUC.

Classic urothelial carcinoma component is present in the majority of the cases, however pure PUCs were also reported. We were not able to demonstrate typical urothelial lesion in this case. PUC infiltrated bladder wall but was covered by normal/reactive urothelium.

Differential diagnostic list should cover:

Plasmacytoma, lymphoma (generally) and chronic inflammatory process. Less important and sometimes morphologically overlapping is lymphoepithelioma-like variant of TCC.

Plasmacytoid variant of TCC is positive for pan-cytokeratin, CK 7; a minority also react with CK 20. Markers like CD138 (plasma cell marker), E-cadherin, p63, uroplakin 3 have also reported to be positive, as well as estrogen and progesterone receptors.

Prognosis is mostly bad with high rate of recurrence. Aggressive behavior is very common. Over 95% of PUC are locally advanced, mostly with lymph node involvement in time of diagnosis.

Selected References:

- 1, Zukergerg LR, Harris NL, Young RH. Carcinomas of the urinary bladder simulating malignant lymphoma. A report of five cases. *Am J Surg Pathol* 1991;15:569-576
- 2, Mai KT, Park PC, Yazdi HM, et al: Plasmacytoid urothelial carcinoma of the urinary bladder. Report of seven new cases. *Eur Urol* 2006;50:1111-1114
- 3, Baldwin L, Lee AHS, Al-Talib RK, et al. Transitional cell carcinoma of the bladder mimicking lobular carcinoma of the breast: a discohesive variant of urothelial carcinoma. *Histopathology* 2005;46:50-56
- 4, Ricardo-Gonzalez RR, Nguyen M, Gokden N, et al. Plasmacytoid carcinoma of the bladder: a urothelial carcinoma variant with a predilection for intraperitoneal spread. *J Urol* 2012;187:852-855
- 5, Patriarca C, Di Pasquale M, Giunta P, et al. CD138-positive plasmacytoid urothelial carcinoma of the bladder. *Int J Surg Pathol* 2008;16:215-217
- 6, Amin MB, Grignon DJ, Srigley JR, Eble JN. *Urological Pathology*, Wolters Kluwer, Philadelphia, 2014
- 7, Moch H, Humphrey PA, Ulbright TM, Reuter VE. *WHO Classification of Tumours of the Urinary System and male Genital Organs*. ICARC, Lyon, 2016

AMR Seminar #69

Case – 7

Contributed by: Jason Hornick, M.D., Ph.D.

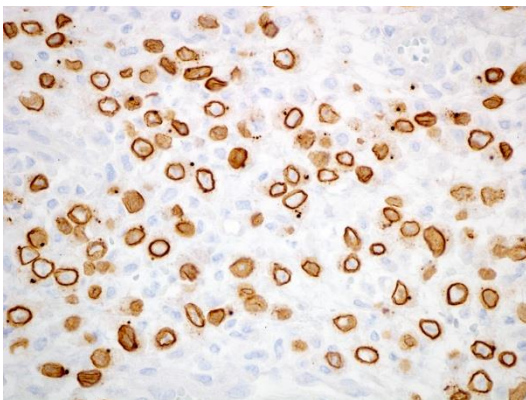
Case History: A 31-year-old man presented with one week of abdominal pain and intermittent vomiting and diarrhea. CT scan showed a large intra-abdominal mass causing small bowel obstruction along with multiple mesenteric, hepatic and adrenal lesions. A partial small bowel resection and right hemicolectomy were performed.

Pathologic Features: A 13-cm mass was identified centered in the mesentery of the small intestine invading into the lumen, as well as a separate 7-cm mass in the pericolonic fat, along with innumerable nodules in the omentum and the serosa of the small intestine and colon. The tumor is composed of sheets of predominantly epithelioid cells with vesicular nuclei, prominent nucleoli, and amphophilic cytoplasm, embedded in a variably prominent myxoid stroma containing inflammatory cells (mostly lymphocytes with few neutrophils and eosinophils). In some areas, the tumor cells are spindled and arranged in loose fascicles. By immunohistochemistry, the tumor cells are positive for desmin, CD30, and ALK, the latter with a nuclear membrane pattern of staining.

Diagnosis: Epithelioid inflammatory myofibroblastic sarcoma.

Comment: This distinctive aggressive variant of inflammatory myofibroblastic tumor has a predilection for the mesentery and omentum, usually affects young men, and often presents with disseminated intra-abdominal metastases. In addition to the unusual epithelioid cytomorphology, myxoid stroma and prominent neutrophils are characteristic features. The unique nuclear membrane pattern of ALK staining correlates with a *RANBP2-ALK* fusion gene. Notably, targeted therapy directed against ALK (e.g., crizotinib) has shown promise in aggressive examples of inflammatory myofibroblastic tumor; the first patient treated in this fashion in fact had an epithelioid inflammatory myofibroblastic sarcoma.

ALK



References

1. Butrynski JE, D'Adamo DR, Hornick JL, et al. Crizotinib in ALK-rearranged inflammatory myofibroblastic tumor. *N Engl J Med*. 2010;363:1727-33.
2. Kimbara S, Takeda K, Fukushima H, et al. A case report of epithelioid inflammatory myofibroblastic sarcoma with RANBP2-ALK fusion gene treated with the ALK inhibitor, crizotinib. *Jpn J Clin Oncol*. 2014;44:868-71.
3. Mariño-Enríquez A, Wang WL, Roy A, et al. Epithelioid inflammatory myofibroblastic sarcoma: An aggressive intra-abdominal variant of inflammatory myofibroblastic tumor with nuclear membrane or perinuclear ALK. *Am J Surg Pathol*. 2011;35:135-44.
4. Mossé YP, Lim MS, Voss SD, et al. Safety and activity of crizotinib for pediatric patients with refractory solid tumours or anaplastic large-cell lymphoma: a Children's Oncology Group phase 1 consortium study. *Lancet Oncol*. 2013;14:472-80.
5. Rafee S, Elamin YY, Joyce E, et al. Neoadjuvant crizotinib in advanced inflammatory myofibroblastic tumor with ALK gene rearrangement. *Tumori*. 2015;101:e35-9.

AMR Seminar #69

Case – 8

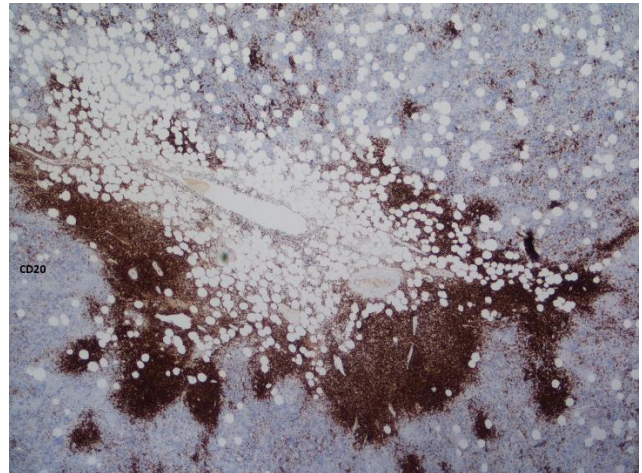
Contributed by: Janez Lamovec, M.D.

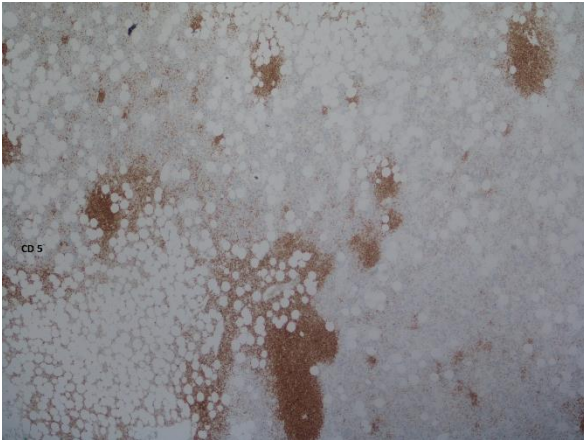
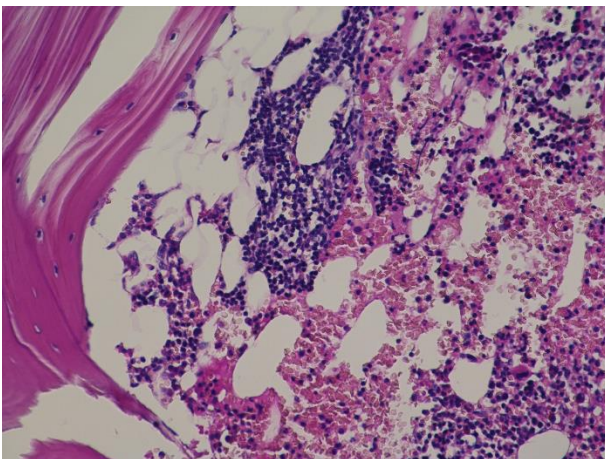
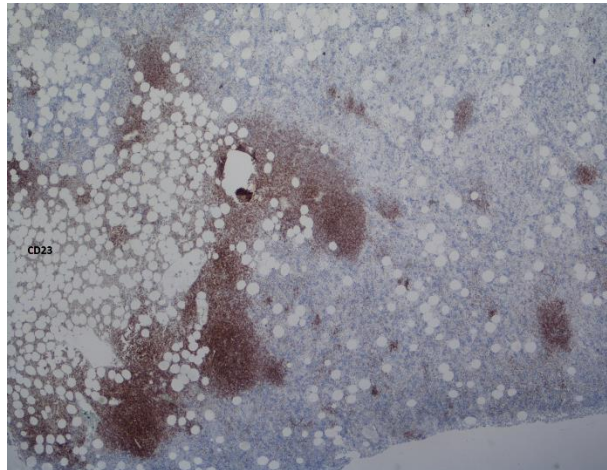
(Case contributed by Dr. Olga Blatnik)

Case History: A 67-year-old man presented with a longstanding abdominal pain and fullness. A mass on the right side of abdomen was palpated. CT showed a fatty, 16.5 x 10 cm retroperitoneal tumor that was diagnosed on core needle biopsy as a myelolipoma. Tumor was resected.

Pathologic findings: Grossly, the tumor measured 21 x 8 x 7 cm and weighed 614 grs. On cut surface, it was soft, reddish-brown in color, and focally yellowish. It was well demarcated with thin fibrous capsule and fat and some muscle tissue on its surface (Fig 1.). Microscopically, the tumor was composed of varying amounts of mature adipose tissue and hematopoietic elements resembling normal bone marrow with trilineage hematopoiesis. In addition, scattered aggregates of uniform small lymphocytes were also present throughout the lesion. Immunohistochemically, lymphocytic cells were positive for CD20 (Fig 2.), CD5 (Fig 3.), CD23 (Fig 4.), bcl2, CD79a and PAX-5 and negative for CD3, CD10, CD21, CD30, cyclin D1, bcl6. Subsequently, bone marrow trephine biopsy was performed that showed foci of similar, mainly perivascular nodular lymphocytic infiltrates with identical immunohistochemical characteristics as those in the retroperitoneal tumor (Fig 5.). Flow cytometry of bone marrow demonstrated a monoclonal lambda positive B cell population comprising 48 % of lymphocytic cells. Molecular genetic test of retroperitoneal lesion confirmed the B cell monoclonality of lymphocytes showing IgH gene rearrangement.

CD20



CD5**CD23**

Diagnosis: Myelolipoma, retroperitoneal, with infiltrates of small B-cell lymphoma of CLL type.

Follow up: The patient shows no B symptoms. Diagnostic work-up did not reveal any abnormality in the peripheral blood, and no evidence of lymphoma elsewhere; no specific treatment has been introduced and only observation was recommended.

Comment: The submitted case is not a diagnostic challenge. Tumor was extraadrenal what is less common, although a number of such locations were described in the literature (presacral area, retroperitoneum, omentum, mediastinum, lung, kidney, stomach). Association of myelolipoma with other tumors has also been reported (with adrenal neoplasms – cortical adenoma, carcinoma, pheochromocytoma, ganglioneuroma), with renal and colon carcinoma, and also, though very rarely, with lymphomas, such as Hodgkin's lymphoma (in renal transplant patient) and SLL/CLL type lymphoma. The association of myelolipoma and malignant lymphoma is most likely coincidental and not the result of a potential malignant transformation of one of the composing elements (lymphocytic cells). Another point to be addressed in cases of myelolipoma associated with lymphoma, particularly small cell lymphoma, is to discriminate the lymphoma infiltrates from reactive lymphocytic infiltrates that may also be found in the bone marrow; the latter, however, are composed of polyclonal B-cells. In the submitted case, monoclonality of B cells was demonstrated in lymphocytes of infiltrates in the retroperitoneal tumor as well as in bone marrow.

References:

O'Malley DP. Benign extramedullary myeloid proliferations. *Mod Pathol* 2007; 20: 405-15.

Gheith S. et al. Small lymphocytic lymphoma/CLL in pelvic myelolipoma. *Int J Clin Exp Pathol* 2009; 2: 95-98.

Noll A. et al. Low grade B cell lymphoma arising in a background of multifocal extra-adrenal myelolipoma. *Ann Clin Lab Sci* 2013; 43: 441-446.

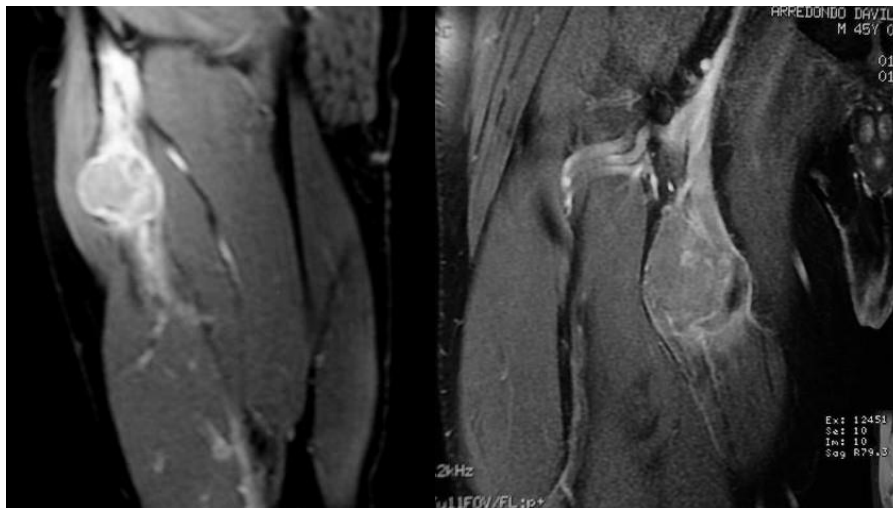
Hagspiel KD. Et al. Manifestation of Hodgkin's lymphoma in an adrenal myelolipoma. *Eur Radiol* 2005; 15: 1757-59.

AMR Seminar #69

Case – 9

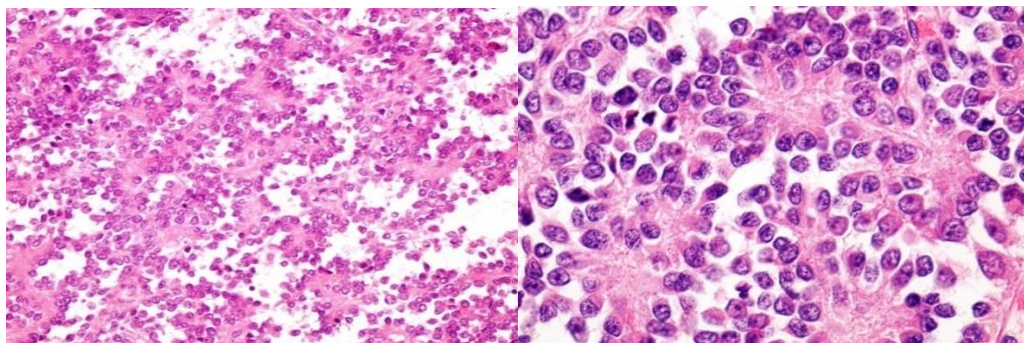
Contributed by: Hugo Domínguez Malagón, M.D.

Case History: One year ago (May 2015), a 45 year-old male noticed a soft tissue tumor in the deep soft tissue of the anterior part of the thigh. The non-painful mass grew progressively in approximately two months. A MR scan revealed a well demarcated 5 cm tumor in the anterior compartment of the right thigh related to the femoral nerve (Fig)

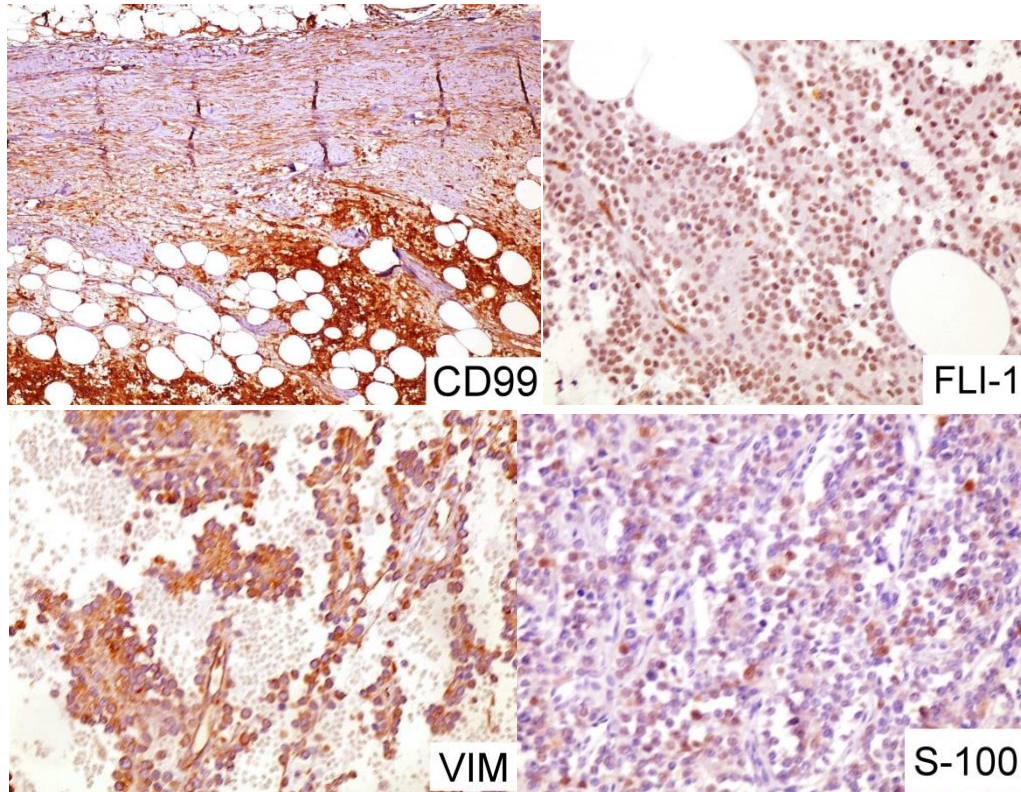


A Tru-cut biopsy was performed and revealed a round cell malignant neoplasm that expressed CD99, FLI-1 vimentin, and a proliferation index of 15% using Ki 67. The tumor cells were negative for CD34 and desmin. A bone marrow biopsy was performed and interpreted as negative. The tumor progressed despite chemotherapy according to the diagnosis. A compartementectomy was then performed; the tumor was well demarcated, friable, whitish gray, surrounding the femoral vessels.

Histology: The neoplasm is composed of small round or pear-shaped cells arranged in a pseudopapillary or pseudo-alveolar pattern and forms perivascular pseudo-rosettes and structures resembling true Homer-Wright rosettes (Figs below). There was a high nuclear/cytoplasmic ratio, granular chromatin and apparent nucleoli; mitoses averaged 20 per 10 HPF. No necrosis was found.

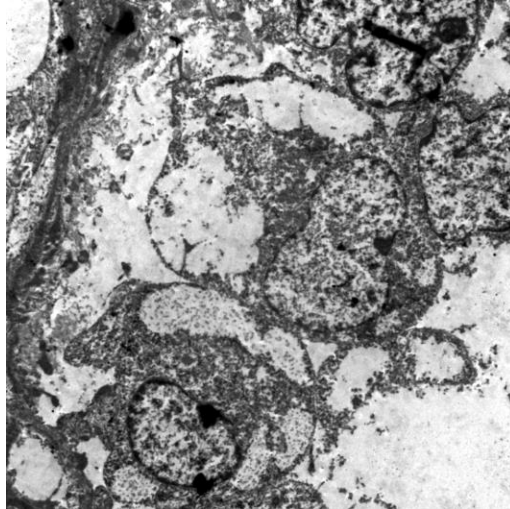


Immunohistochemistry. The cells were positive for CD99 (stronger in the rosette-like structures, vimentin, FLI-1 and S100. They were negative for CD34, TLE-1, EMA, CD10, CK AE1-AE3, desmin, TdT, CD56, CD57, synaptophysin and GFAP.

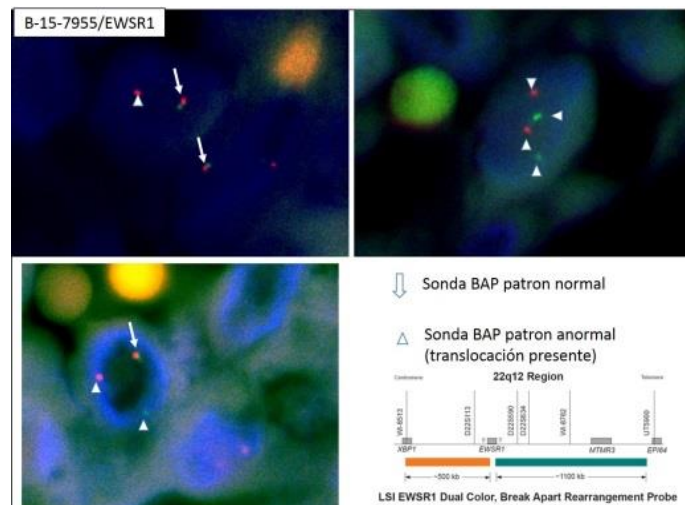


Ultrastructure

Small round or polygonal cells with moderate amount of cytoplasm containing abundant glycogen, round nuclei with fine chromatin and peripherally located small nucleoli. No cell processes, axons or neurosecretory granules were found.



Molecular Studies. FISH performed twice (one in Wisconsin by courtesy of Saul Suster) using a DNA probe for EWSR-1 shows a split-apart signal in 82% of the cells, consistent with rearrangement.



DIAGNOSIS: Neuroblastoma-like Ewing sarcoma? or pseudorosette-forming Ewing sarcoma? or peripheral nerve/PNET? or neuroblastoma-like MPNST or what?

DISCUSSION

The presence of *EWSR/FLI-1 t(11;22)(q24;q12)* is considered diagnostic of Ewing /PNET family of tumors (EFT), it is detected by RT-PCR but EWSR-1 demonstrated by FISH plus CD99 and FLI-1 by IHC are regarded as enough evidence for the same purpose. This “family” has many members like: adamantinoma-like Ewing sarcoma, PNET with neuroendocrine differentiation, basaloid phenotype, myoepithelioid phenotype, associated to nerves, S-100 positive tumors, polyphenotypic tumors mixed with ARMS, etc.

These tumors affect almost all ages and many anatomical sites and can vary in biological behavior and response to treatment with chemo or radiotherapy. To make matters worse, tumors sharing the same location, morphology and immunophenotype have been called “Ewing-like adamantinoma” when negative for the translocation, and “adamantinoma-like Ewing tumor” when positive.

EWSR1 is a “promiscuous” gene fused to many partners and expressed by a wide variety of tumors (like myoepithelial tumors and others).

The present case is a peculiar one, the patient is 45, MR shows a well delimited tumor associated to femoral nerve (by three different groups of radiologists), does not have necrosis, and progressed despite the chemotherapy.

The philosophical question is: is the genotype a real “gold standard” that defines a single entity with many phenotypes? Or the opposite: is the genotype shared by many entities affecting different age groups, associated to diverse structures, and with dissimilar response to treatment?

Pathologists and oncologists will need to decide what is more important. Your opinion as to how best to categorize this tumor will be appreciated.

AMR Seminar #69

Case – 10

Contributed by: Michal Michal, M.D. (Case nr. M87844/10)

History: The patient was a 41 year old woman with a tumor of the ovary 2 cm in size. Most of the tumor, particularly the spindle cell part, was immunohistochemically positive with antibodies to inhibin, calretinin and some part was cytokeratin positive. The eosinophilic hepatic cells were Hep-Par-1 and Arginase-1 positive, in addition to positivity to wide spectrum cytokeratins

Diagnosis: Granulosa cell tumor of the ovary with true hepatic differentiation.

References

1. Nogales FF, Concha A, Plata C, Ruiz Avila I. Granulosa cell tumor of the ovary with diffuse true hepatic differentiation simulating stromal luteinization. Am J Surg Pathol 1993;17:85-90.
2. Ahmed E, Young RE, Scully RE. Adult granulosa cell tumor of the ovary with foci of hepatic cell differentiation. A report of four cases. Am J Surg Pathol 1999;23: 1089-1093

AMR Seminar #69

Case – 11

Contributed by: Michal Michal, M.D. (Case nr. M27261/13)

History: The patient was a 53 year old man with a tumor of the paratestis, 3 cm in size. The lesion revealed cystadenomatous change. Grossly, the tumor had an elastic consistency and was white in color. Neither necrosis nor hemorrhage were evident on the cut surface. Histologically the tumor reveals serous epithelium similar to the one that can be found in the fallopian tubes and in part of the tumor there is a spindle cell stroma that is indistinguishable from the stroma of the ovary. The tumor is identical to Cases 1 and 2 of the paper we recently published (1).

Diagnosis: Cystadenoma of paratestis with ovarian stroma (mixed epithelial and stromal tumor of the testis)

Reference

1. Michal M, Kazakov VD, Kacerovska D, Kuroda N, Lovric E, Wachter DL, Agaimy A, Hes O.: Paratesticular cystadenomas with ovarian stroma, metaplastic serous Müllerian epithelium and male adnexal tumor of probable Wolffian origin. A series of 5 hitherto poorly recognized testicular tumors. Annals of Diagnostic Pathology 2013;17:151-158.

AMR Seminar #69

Case – 12

Contributed by: Markku Miettinen, M.D.

History: 39-year-old woman had surgery for a recurrent nodule in the shoulder, about 2 cm in diameter.

Diagnosis: Chondroid lipoma, recurrent.

Discussion: Chondroid lipoma is a very rare histologically distinctive lipomatous tumor originally reported by Meis and Enzinger in AFIP in 1993 with perhaps <100 cases reported to date. It occurs in adult patients at a variety of peripheral soft tissue sites but has also been reported in the tongue, among others. This tumor can be subcutaneous or intramuscular. It is a non-malignant tumor but can recur locally. Histology includes epithelioid cells in a chondroid matrix, with low mitotic activity. Tumor contains fatty differentiation that is evident in some of the epithelioid cells, often with multivacuolated lipoblast-like appearances. There are also intermingled mature appearing fat cells. Hyalinized or even calcified areas can be present. Some variants may simulate extraskeletal myxoid chondrosarcoma, especially in small biopsy, if fatty differentiation is not obvious. C11orf95-MKL2 has been reported as an oncogenic gene fusion corresponding to the t(11;16)(q13;p13) translocation in chondroid lipoma.

References:

Meis JM, Enzinger FM. Chondroid lipoma. A unique tumor simulating liposarcoma and myxoid chondrosarcoma. Am J Surg Pathol. 1993 Nov;17(11):1103-12.

Huang D, Sumegi J, Dal Cin P, Reith JD, Yasuda T, Nelson M, Muirhead D, Bridge JA. C11orf95-MKL2 is the resulting fusion oncogene of t(11;16)(q13;p13) in chondroid lipoma. Genes Chromosomes Cancer. 2010 Sep;49(9):810-8.

AMR Seminar #69

Case – 13

Contributed by: Cesar Moran, M.D.

Clinical History: 19-year-old young man presents with swelling of the left testicle and a mass is detected. Left orchiectomy was performed.

I would like to know the members' opinion on the interpretation of this tumor.

AMR Seminar #69

Case – 14

Contributed by: Vania Nosé, M.D., Ph.D.

Clinical History: This is a 45 year old gentleman who has had a long history of care at our hospital. He has a history of bilateral neck tumors, which were addressed surgically on the left side with a surgical approach in the 1980s, as this involves the vagale and the jugular foramen. He then had radiation therapy afterwards. His disease has been stable for many years. He has had multiple adjuvant procedures including a Montgomery thyroplasty. He likewise underwent a gracilis flap reconstruction on the left side five years ago. He has overall been stable and has not followed up in a bit of time. Recently, he presented with a sense of heart palpitation and discomfort in the chest and underwent a full ER evaluation. This included a neck and chest CT which noted a large mass in the lower neck extending into the mediastinum. There is no previous radiographic evaluation to cover this area that is immediately accessible. He does report having some mild fluctuations in his voice and some issues with swallowing, which are extensions of his long-standing issues. Further studies confirmed two distinct masses, one in the left neck extending to superior mediastinum, and other in a periaortic location. He was submitted to surgery for removal of both tumors.

Pathological Findings: We received two specimens from his left neck and chest mass (5.6 cm) and from his periaortic mass (2.6 cm).

Microscopically, both tumors were cellular and contained islands of neoplastic cells surrounded by a lymphoplasmacytic-rich fibrovascular core. There were areas of fibrosis and hyalinization. No increased mitotic activity or significant pleomorphism were identified. The lesion extended to the inked tissue edges.

The internal positive controls for SDHB, as endothelial cells and sustentacular cells, showed preserved granular cytoplasmic staining SDHB immunostaining. Loss of staining was found in the tumor cells.

Diagnosis: Hereditary multicentric paraganglioma-pheochromocytoma syndrome due to mutation of SDH gene.

Discussion: Pheochromocytomas and paragangliomas are tumors of neural crest origin that arise from cells of the adrenal medulla or paraganglia, respectively. Paragangliomas can be subdivided according to their location. Head and neck paragangliomas arise from parasympathetic paraganglia and are almost always nonfunctioning. In contrast, paragangliomas located below the neck arise from sympathetic paraganglia and thus are often symptomatic secondary to catecholamine production. Both pheochromocytomas and paragangliomas can be sporadic or can arise as part of a hereditary tumor syndrome, such as multiple endocrine neoplasia type 2, von Hippel Lindau (VHL) disease, neurofibromatosis type 1, Carney-Stratton syndrome, hereditary syndromes associated with genes KIF1BB, MAX, TMEM127, EGLN1, and hereditary paraganglioma-pheochromocytoma syndrome SDH-related (HPGL/PCC).

Succinate dehydrogenase (SDH) is an enzyme complex localized to the inner mitochondrial membrane that plays an integral role in cellular metabolism. It is a member of both the Krebs cycle and the electron transport chain (known as complex II), catalyzing the oxidation of succinate to fumarate and coupling this reaction to the reduction of ubiquinone. SDH is a heterotetrameric complex composed of 4 protein subunits (A, B, C, and D). SDHA and B form the catalytic core, whereas SDHC and D anchor the complex to the inner mitochondrial membrane.

The SDH genes act as tumor suppressor genes: tumors demonstrate loss of heterozygosity in combination with germline-inactivating mutations. This results not only in a lack of SDH enzyme activity, but also in destabilization of the SDH protein complex (consequently "SDH-deficient"). Destabilization of the complex, as a result of a mutation in

any of the 4 SDH genes, can be identified by immunohistochemical analysis for SDHB. SDH-deficient tumors lack SDHB expression by immunohistochemistry.

One notable aspects of the discovery of SDH mutations in pheochromocytomas and paragangliomas is the high frequency of germline mutations in these tumors, especially paragangliomas, in which the rate of SDH mutations has been reported as high at 54%. Although patients harboring germline SDH mutations are more likely to develop pheochromocytomas at a younger age and have a higher incidence of bilateral disease, clinical history can be confusing.

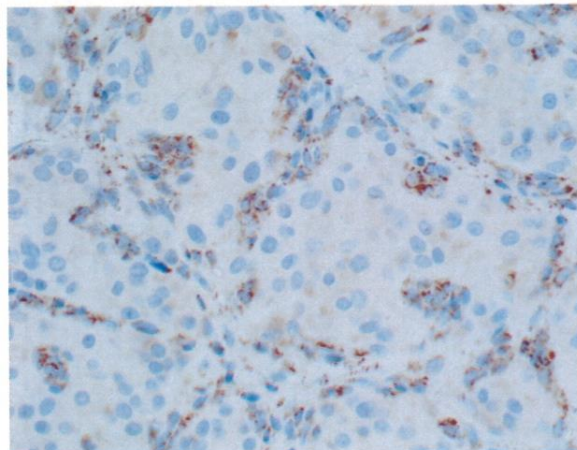
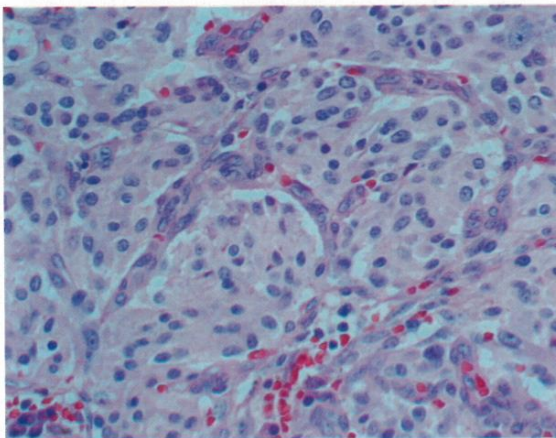
Head and neck paragangliomas account for the majority of paragangliomas, and a striking number of these tumors harbor SDH germline mutations. SDHD mutations are the most frequent SDH mutations in patients with head and neck paragangliomas. Patients harboring germline mutations in SDHD are more likely to have multifocal disease compared with patients with SDHB and SDHC mutations. Although patients with a positive family history have a very high rate of SDHD mutation, SDHD mutations also occur in apparently sporadic head and neck paragangliomas.

Although thoraco-abdominal paragangliomas are not nearly as common as pheochromocytomas and head and neck paragangliomas, the higher rate of malignancy in these tumors imparts them with clinical significance. We now know that the frequency of specific SDH mutations likely contributes to the higher rate of malignancy in paragangliomas at these sites. In thoraco-abdominal paragangliomas SDHB mutations predominate.

Identifying SDHB mutations in paragangliomas and pheochromocytomas is important not only timely to genetic counseling, but also due to the fact that the SDHB mutation status has prognostic implications. SDHB mutations correlate with malignant behavior in both paragangliomas and pheochromocytomas.

Although immunohistochemical staining for SDHB is high effective for identifying SDH-deficient tumors, caution regarding the interpretation of this stain is warranted. SDH complex is located in mitochondria, so, intact staining is cytoplasmic and granular.

Loss of staining in tumors should always be interpreted in the context of internal positive controls. In paragangliomas and pheochromocytomas, endothelial cells and non-neoplastic sustentacular cells will retain SDHB expression. Once a tumor is found to be SDH deficient, mutation analysis needs to be performed to evaluate for the presence of a germline SDH mutation.



AMR Seminar #69

Case – 15

Contributed by: Kyle Perry, M.D.

History: This patient is a 52 y/o female who had a three-year history of a right nasal obstruction that did not improve with nasal steroids. Radiologic examination revealed an opacification of the right nasal cavity that was thought to reflect sinonasal polyposis (Fig. 1). An endoscopic biopsy was performed.

Pathologic Findings: The sections of the mass showed a moderately cellular spindle cell neoplasm arranged around glands lined by respiratory epithelium (Fig. 2a). The tumor cells exhibit a pattern of short and long fascicles (Fig. 2b). Rare areas of nuclear “buckling” are present (Fig. 2c), and there are foci of a prominent “hemangiopericytoma-like” vascular pattern (Fig. 2d).

Immunohistochemical stains show the tumor cells to exhibit expression of S-100 (Fig. 3a) and SMA (Fig. 3b). The cells in this particular case were also positive for CD34, bcl-2, and were negative for SOX-10 (not shown).

Fluorescent in-situ hybridization studies revealed a break in the PAX-3 probe, consistent with a translocation involving the *PAX-3* gene.

Diagnosis: Biphenotypic sinonasal sarcoma.

Discussion: Biphenotypic sinonasal sarcoma is a recently described entity that arises in the sinonasal region in adults. This particular case exhibits many of the morphologic characteristics noted in the first case series, namely a fascicular arrangement of bland appearing spindled cells, focal nuclear buckling, and a hemangiopericytoma-like vascular pattern. (2) These tumors characteristically express S-100 and SMA but lack staining with SOX-10. Some cases will have epithelioid rhabdomyoblastic like cells that can stain positive for desmin and MyoD1. Occasional cases have been shown to have focal positivity for CD34 and AE1/AE3. (1) These neoplasms have been found to commonly exhibit rearrangements of *PAX3*. Identified fusion partners include *MAML3*, *NCOA1* and *FOXO1* (1,3,4). The *PAX3-FOXO1* fusion is particularly interesting as this fusion gene also occurs in alveolar rhabdomyosarcoma. (4)

Given the spindled and fascicular nature of biphenotypic sinonasal sarcoma, the differential includes a low-grade malignant peripheral nerve sheath tumor and monophasic synovial sarcoma. A pathologist could be enticed to make an erroneous diagnosis of synovial sarcoma based on a fascicular spindled architecture and a positive TLE-1 stain (which can occur in biphenotypic sinonasal sarcoma). (4) Positive S-100 staining of these entities could deceive the pathologist to mistake this neoplasm for a low-grade malignant peripheral nerve sheath tumor.

In the initial case series, almost half (44%) experienced at least one recurrence. No patients have been found to have metastasis or have died from this neoplasm. (2) To date, this particular patient has not developed recurrence since the initial procedure (January 2014).

Dr. Karen Fritchie gave a very nice presentation regarding this entity at the recent USCAP Bone and Soft Tissue Pathology Evening Specialty Conference, and I thought that this case would make a nice edition to the AMR collection.

When I first encountered this case, I thought that it was likely a low-grade malignant peripheral nerve sheath tumor. I sent it to Dr. Christopher Fletcher, who made the correct diagnosis. With the recent publications noting the translocation involving the *PAX3* gene, I recently sent the case to Dr. Julie Bridge, who found the break in the corresponding probe. Special thanks for their assistance with this case.



Fig. 1. The CT scan shows a mass in the right nasal cavity.

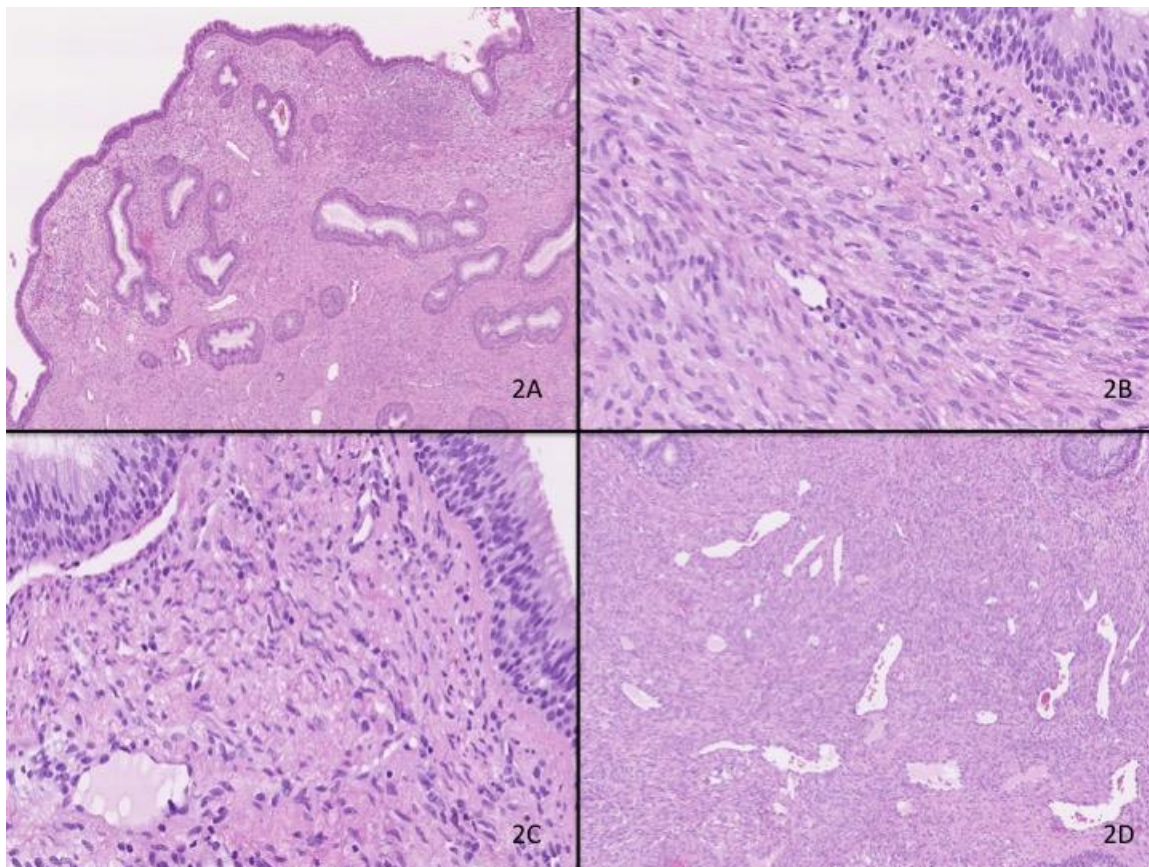


Figure 2a-2d. The section of the polypoid lesion showed spindle cells intimately associated with respiratory mucosa (2a). The cells are arranged in short and long fascicles (2b). Rare areas of nuclear "buckling" are noted (2c). A staghorn vascular pattern is present (2d).

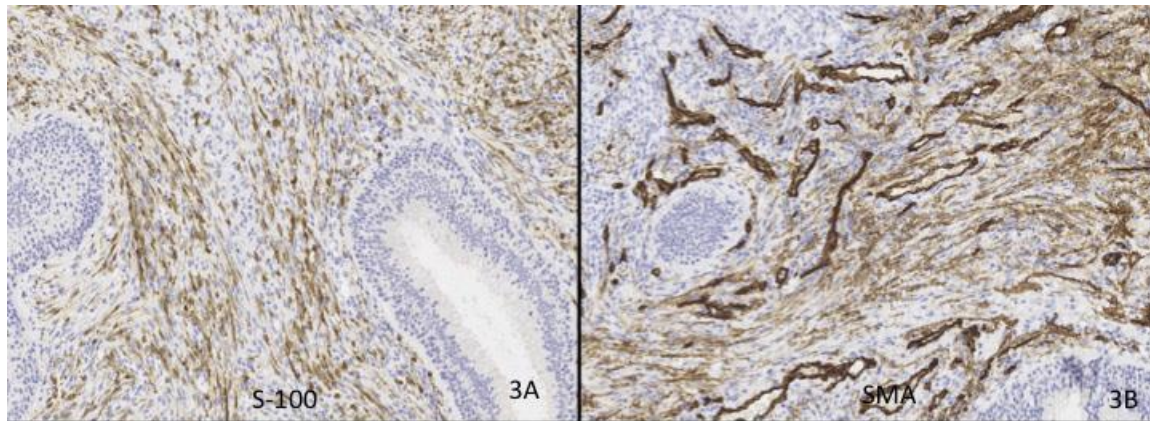


Figure 3a-3b. The spindled cells are positive for S-100 (Fig. 3a) and SMA (Fig. 3b).

References

1. Huang SC, Ghossein RA, Bishop JA, et al. Novel PAX3-NCOA1 Fusions in Biphenotypic Sinonasal Sarcoma With Focal Rhabdomyoblastic Differentiation. *Am J Surg Pathol* 2016;40:51-59.
2. Lewis JT, Oliveira AM, Nascimento AG, et al. Low-grade sinonasal sarcoma with neural and myogenic features: a clinicopathologic analysis of 28 cases. *Am J Surg Pathol* 2012;36:517-525.
3. Wang X, Bledsoe KL, Graham RP, et al. Recurrent PAX3-MAML3 fusion in biphenotypic sinonasal sarcoma. *Nat Genet* 2014;46:666-668.
4. Wong WJ, Lauria A, Hornick JL, et al. Alternate PAX3-FOXO1 oncogenic fusion in biphenotypic sinonasal sarcoma. *Genes Chromosomes Cancer* 2016;55:25-29.

AMR Seminar #69

Case – 16

Contributed by: Kyle Perry, M.D.

History: This patient is a 56 y/o female with a left scalp lesion. She has a history of pancreatic cancer and had a bone marrow transplant in 2014 for acute myeloid leukemia. A punch biopsy was performed.

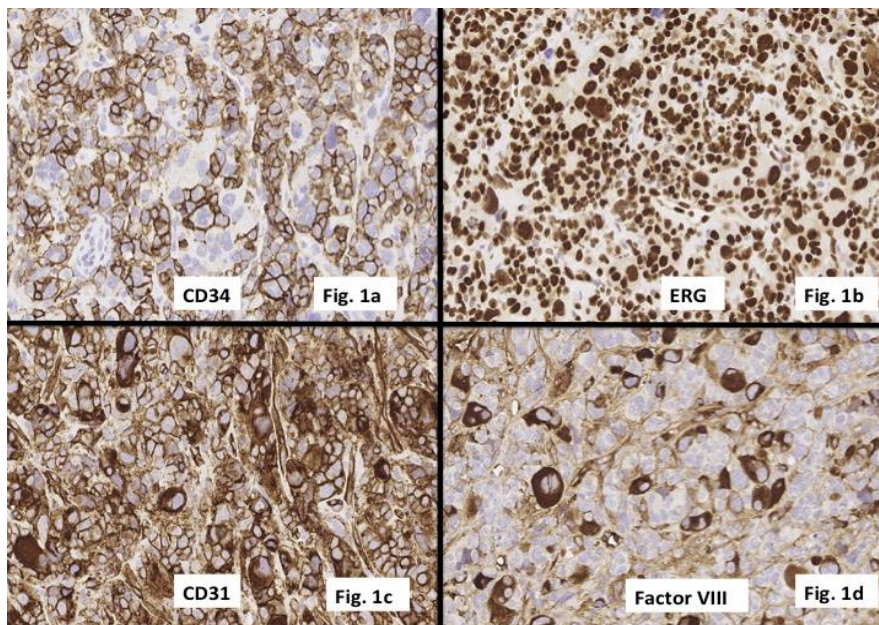
Pathologic Findings: The sections of the lesion show epithelioid and pleomorphic tumor cells with enlarged nuclei and prominent nucleoli. Scattered "giant cells" with hyperchromatic nuclei are present. Bizarre mitosis are also noted.

Immunohistochemical stains show the tumor cells to be positive for CD34 (Fig. 1a), ERG (Fig. 1b), CD31 (Fig. 1c) and factor VIII (Fig. 1d). However, the neoplastic cells are also positive for myeloperoxidase (Fig. 2a), CD45 (Fig. 2b), CD117 (Fig. 2c), and CD43 (Fig. 2d).

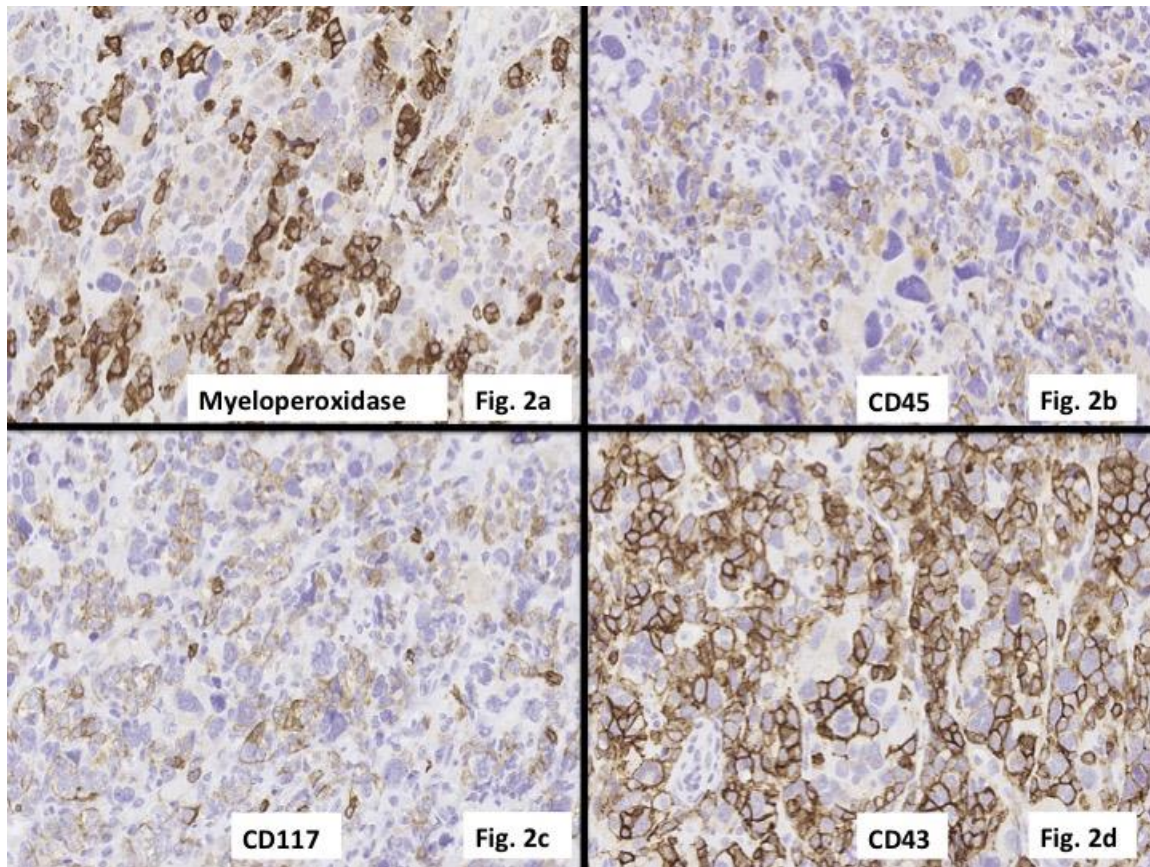
Diagnosis: Myeloid sarcoma.

Discussion: Although not extraordinarily rare, I thought that this was a nice case that illustrated the deceptive potential of myeloid sarcomas, particularly if the pathologist is not privy to the patient's clinical history. In this particular case, the tumour cells stained with CD34, ERG, and CD31. Factor VIII highlighted megakaryocytes. This pattern could be mistaken for epithelioid angiosarcoma. The tumor cells, however, were positive for granulocytic markers such as CD117, CD45, myeloperoxidase and CD43, revealing this neoplasm's true colors.

Myeloid sarcomas are malignant neoplasms composed of myeloblasts or immature myeloid cells in extramedullary sites or bone. These can occur concurrently with AML or a myeloproliferative disorder. These can also be the sentinel manifestation of acute myeloid leukemia in a patient. The differential diagnosis includes small cell malignancies (such as Ewing sarcoma), undifferentiated carcinoma or other hematopoietic neoplasms (such as Hodgkin lymphoma). Of interest, this particular tumor was positive for epithelial markers (AE1/AE3, Cam 5.2). (1,2)



Figures 1a-1d. The tumor cells were positive (in varying degrees) for numerous endothelial markers, including CD34, ERG, CD31 and Factor VIII.



Figures 2a-2d.

Additional granulocytic markers (myeloperoxidase, CD45, CD117 and CD43) revealed the true nature of this myeloid sarcoma.

References

1. Alexiev BA, Wang W, Ning Y, et al. Myeloid sarcomas: a histologic, immunohistochemical, and cytogenetic study. *Diagn Pathol* 2007;2:42.
2. Audouin J, Comperat E, Le Tourneau A, et al. Myeloid sarcoma: clinical and morphologic criteria useful for diagnosis. *Int J Surg Pathol* 2003;11:271-282.

AMR Seminar #69

Case – 17

Contributed by: Fredrik Petersson, M.D.

Clinical History: A 77 y/o man presented with a slow growing, painless lump in the left submandibular region. The case was sent to me as a consult since the pathologists at the original hospital could not agree on whether it was benign or malignant.

Pathologic Findings: The tumor shows a multinodular architecture displaying tubular, solid and focally cystic patterns. There is a distinct biphasic (epithelial and myoepithelial) cellular composition (highlighted by the provided IHC stains; EMA, SMA, p63, CK14 and S-100 protein) with several areas of “myoepithelial overgrowth”. The cytological nuclear atypia is generally low-grade, with a few microscopic foci where the epithelial component shows slightly increased nuclear atypia, which, however, does not warrant a designation of “high-grade transformation”. As mentioned above there is a multinodular structure of the tumor with shows a low-grade (“bulky pattern”) of invasion. The mitotic activity is variable, albeit significant, but does not exceed 10/10 HPFs. There is no necrosis and I have seen no perineural spread. IHC (Ki-67) shows a somewhat variable proliferation rate, approximately 15%. The background salivary gland parenchyma exhibits moderate chronic inflammation with marked atrophy and lipomatous metaplasia.

Diagnosis: Epithelial-myoepithelial carcinoma with multifocal myoepithelial overgrowth.

Comments: This is (again), not an earth-shattering case, but an uncommon low-grade salivary gland malignancy (representing no more than 1% of salivary gland neoplasms), which may be difficult to recognize as a carcinoma (vide infra) and also which also may display a range of histological appearances which exhibits overlapping features with other salivary gland tumors, and for these reasons is worth sharing and discussing with the members of the club. Epithelial-myoepithelial carcinoma (EMC) was already defined as an entity in 1972.¹ It occurs slightly more frequently among women and has, as many LG-SG carcinomas, a wide reported age span (6-92 years), but is most commonly seen in the 6-7th decade.¹ The majority (60-80%) of EMC occurs in the parotid, but may also involve the submandibular glands and minor SG, including sites throughout the upper aerodigestive tract (sinonasal tract, oropharynx, larynx, trachea, bronchus and lacrimal gland).^{5, 1, 6, 1, 4} EMC has a nodular, multinodular pattern of growth and as such is most commonly well delineated. Moreover, 25-30% of EMC are at least partially encapsulated.¹ This “bulky – lobulated” pattern of invasion can give rise to difficulties in interpretation and differs from many other LG-SG carcinomas. This notwithstanding, up to 30% of EMCs may show perineural invasion.¹ This pattern of invasion is typical of EMC may give rise to difficulties in interpretation – and it adds to Goran’s comments on this issue with regards to myoepithelial-rich SG carcinomas in conjunction with David’s case 4 in seminar #66. This growth pattern also helps to distinguish EMC with clear cell myoepithelial overgrowth (as seen in the actual case) from clear cell carcinoma which tend to infiltrate in small nests and strands.⁶ The histological sine qua non in EMC is a biphasic cellular arrangement with in its classic form tubules lined by an inner ductal epithelial layer and an outer clear cell - myoepithelial layer. In addition to a tubular pattern, trabecular, papillary and, uncommonly, cystic arrangements may also be encountered.¹ The latter was present in this case. As in all myoepithelial containing neoplasms, collagenous spherules/crystalloids may be present. Histological variants of EMC have been reported and these include an epithelial component with oncocytic, apocrine, clear cell, sebaceous and mucinous features.¹ Also the myoepithelial cells may display oncocytic changes.⁶ Moreover, the myoepithelial component may show squamous differentiation and what has been referred to as “ancient change”, spindle cell-change and Verocay-like palisading.^{1, 6, 6, 9}

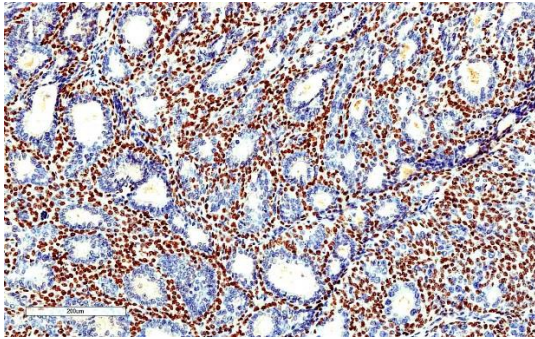
High-grade transformation (“dedifferentiation”) is an increasingly recognized phenomenon in SG neoplasms which I recently reviewed.¹ This is a phenomenon that also occur in EMC. Just over 20 cases of EMC-HGT have been reported. Reportedly, the age at presentation of patients with EMC-HGT is 10-15 years earlier than patients with conventional EMC (70-75 vs 60 years). Akin to cEMC, HGT-EMC most commonly occur in the major (parotid and submandibular) glands. Histologically, EMC-HGT frequently exhibits solid growth with loss of the characteristic biphasic microtopographic arrangements of tumor cells. The neoplastic cells in the HG areas exhibit classical cyto-/histomorphological features of malignancy, including increased nuclear size and pleomorphism, increased nucleolar size, increased mitotic activity and frequently necrosis. In EMC-HGT, the HG component may display either an epithelial

or myoepithelial phenotype and the HG cells may exhibit an epithelioid, plasmacytoid, clear cell, squamous or spindle morphology^{1, 6, 9}. Interestingly, in one case of HGT-EMC, the HG malignant cells displayed two different lines of differentiation; salivary duct carcinoma and myoepithelial carcinoma.⁵ HGT-EMC is an aggressive disease and has a 50% risk of lymph node- and 30% risk of distant metastasis.

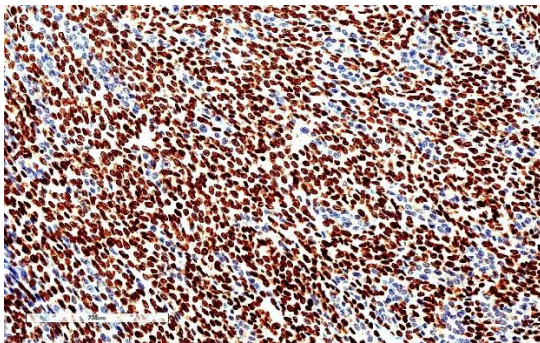
It has been suggested that non-neoplastic – hyperplastic proliferation of intercalated ducts is a precursor to EMC.^{3, 5, 9} Moreover, Yu and Donath published a series of intercalated duct lesions which they termed “adenomatous ductal proliferations”.² Of the 13 cases, 7 (54%) were associated with a salivary gland tumor. Thus, it is conceivable that there may exist a hyperplasia – adenoma – carcinoma sequence for EMC. On this note it is worth to mention that both Chetty and DiPalma have presented cases with clear proliferations in the intercalated ductal lesions adjacent to the EMCs.^{3, 5} However, there may be more to this. In Weinreb’s study, although 19/32 (59%) of IDLs were associated with a tumor, only 3 were EMC and 8 basal cell adenomas, 2 basal cell adenocarcinomas, 2 PAs, 2 mucoepidermoid carcinomas, 1 Warthin tumor and one acinic cell carcinoma.⁹

P63 from areas without (A) and with (B) myoepithelial overgrowth.

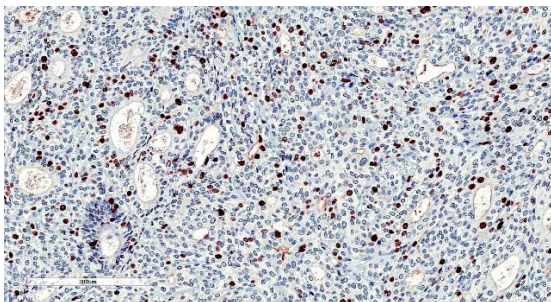
A.



B.



Ki-67 labelling exceeds that what is expected in a benign salivary gland tumor.



References:

1. Donath K, Seifert G, Schmitz R. [Diagnosis and ultrastructure of the tubular carcinoma of salivary gland ducts. Epithelial-myoepithelial carcinoma of the intercalated ducts]. *Virchows Arch A Pathol Pathol Anat.* 1972;356:16-31.
2. Seethala RR, Barnes EL, Hunt JL. Epithelial-myoepithelial carcinoma: a review of the clinicopathologic spectrum and immunophenotypic characteristics in 61 tumors of the salivary glands and upper aerodigestive tract. *Am J Surg Pathol.* 2007;31:44-57.
3. Imate Y, Yamashita H, Endo S, et al. Epithelial-myoepithelial carcinoma of the nasopharynx. *ORL J Otorhinolaryngol Relat Spec.* 2000;62:282-285.
4. Kumai Y, Ogata N, Yumoto E. Epithelial-myoepithelial carcinoma in the base of the tongue: a case report. *Am J Otolaryngol.* 2006;27:58-60.
5. Guan M, Cao X, Wang W, et al. Epithelial-myoepithelial carcinoma of the hypopharynx: A rare case. *Oncol Lett.* 2014;7:1978-1980.
6. Ru K, Srivastava A, Tischler AS. Bronchial epithelial-myoepithelial carcinoma. *Arch Pathol Lab Med.* 2004;128:92-94.
7. Kong SK, Goh EK, Chon KM, et al. Epithelial-myoepithelial carcinoma in the external auditory canal. *Otolaryngol Head Neck Surg.* 2008;139:598-599.
8. Goncalves AC, de Lima PP, Monteiro ML. Epithelial-Myoepithelial Carcinoma of the Lacrimal Gland 14 Years After En Bloc Resection of a Pleomorphic Lacrimal Gland Adenoma. *Ophthalm Plast Reconstr Surg.* 2014
9. Wang B, Brandwein M, Gordon R, et al. Primary salivary clear cell tumors--a diagnostic approach: a clinicopathologic and immunohistochemical study of 20 patients with clear cell carcinoma, clear cell myoepithelial carcinoma, and epithelial-myoepithelial carcinoma. *Arch Pathol Lab Med.* 2002;126:676-685.
10. Seethala RR. Oncocytic and apocrine epithelial myoepithelial carcinoma: novel variants of a challenging tumor. *Head Neck Pathol.* 2013;7 Suppl 1:S77-84.
11. AT S, Salama M. Oncocytic epithelial-myoepithelial carcinoma of the salivary gland; an underrecognized morphologic variant. *Mod Pathol.* 2005.
12. Seethala RR, Richmond JA, Hoschar AP, et al. New variants of epithelial-myoepithelial carcinoma: oncocytic-sebaceous and apocrine. *Arch Pathol Lab Med.* 2009;133:950-959.
13. Shinozaki A, Nagao T, Endo H, et al. Sebaceous epithelial-myoepithelial carcinoma of the salivary gland: clinicopathologic and immunohistochemical analysis of 6 cases of a new histologic variant. *Am J Surg Pathol.* 2008;32:913-923.
14. Roy P, Bullock MJ, Perez-Ordóñez B, et al. Epithelial-myoepithelial carcinoma with high grade transformation. *Am J Surg Pathol.* 2010;34:1258-1265.
15. Petersson F. High-Grade Transformation ("Dedifferentiation") - Malignant Progression of Salivary Gland Neoplasms, Including Carcinoma ex Pleomorphic Adenoma: A Review. . *Pathology Case Reviews* 2015;20:27-37.
16. Baker AR, Ohanessian SE, Adil E, et al. Dedifferentiated epithelial-myoepithelial carcinoma: analysis of a rare entity based on a case report and literature review. *Int J Surg Pathol.* 2013;21:514-519.
17. Chetty R. Intercalated duct hyperplasia: possible relationship to epithelial-myoepithelial carcinoma and hybrid tumours of salivary gland. *Histopathology.* 2000;37:260-263.
18. Di Palma S. Epithelial-myoepithelial carcinoma with co-existing multifocal intercalated duct hyperplasia of the parotid gland. *Histopathology.* 1994;25:494-496.
19. Weinreb I, Seethala RR, Hunt JL, et al. Intercalated duct lesions of salivary gland: a morphologic spectrum from hyperplasia to adenoma. *Am J Surg Pathol.* 2009;33:1322-1329.
20. Yu GY, Donath K. Adenomatous ductal proliferation of the salivary gland. *Oral Surg Oral Med Oral Pathol Oral Radiol Endod.* 2001;91:215-221.

AMR Seminar #69

Case – 18

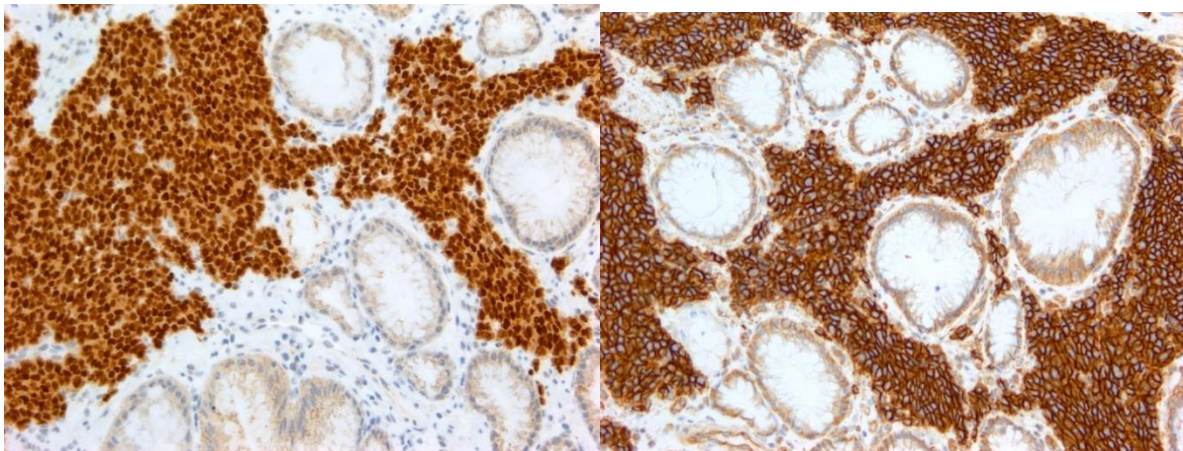
Contributed by: Murray Resnick, M.D.

Case History: The patient is a 63 year old woman who presented with shortness of breath and a hemoglobin of 7.4. EGD revealed a large gastric mass with stigmata of recent bleeding. The diagnosis was made on the initial biopsy. Following the biopsy and an extensive negative radiological work-up distal gastrectomy was performed. The tumor measured 9x6x3cm and involved the full-thickness of the gastric wall extending to the mesothelial lined serosa. Lymph nodes were negative, lymphovascular invasion was detected.

Pathology: Histologically the tumor exhibits a solid growth pattern of monotonous, undifferentiated cells with little cytoplasm. The proliferative rate is very high and areas of geographic necrosis are present. An extensive immunohistochemical work-up was performed and the tumor cells were negative for epithelial, muscle and melanoma markers, synaptophysin, chromogranin, and CD45. The tumor cells were strongly positive for CD99 in a membranous pattern and for NKX2.2 in a nuclear pattern (see below). The Ki-67 labeling index was 70%. FISH studies were positive for the *EWSR1* 22q12 rearrangement in 40% of the cells examined.

Final Diagnosis: Primary Ewing's sarcoma/Primitive neuroectodermal tumor of the stomach.

Discussion: Primary gastric Ewing/PNET sarcomas are very rare with less than 10 case reports published. NKX2.2 is a relatively new immunohistochemical marker useful in the diagnosis of ES/PNET. It is a homeobox transcription factor that plays a crucial role in neural development and is a target gene product of *EWSR1-FLI1* whose expression is upregulated in ES/PNET (1). Yoshida et al were the first to describe the utility of NKX2.2 as a marker of ES/PNET (2). In a more recent study Shibuya et al have shown that the combination of CD99 and NKX2.2 positivity has a 98% specificity for the diagnosis of ES/PNET (3). However, the list of tumors that may exhibit NKX2.2 positivity continues to expand and includes small cell carcinoma (which was in the initial differential diagnosis of this case), mesenchymal chondrosarcoma, olfactory neuroblastoma, Merkel cell carcinoma and others (3, 4) Neuroendocrine carcinoma of the stomach (also in the differential diagnosis of this case) has also shown to be positive (5).



References

1. Smith R, *et al* (2006) Cancer Cell 9:405-416.
2. Yoshida A, *et al* (2012) Am J Surg Path 36:993-999.
3. Shibuya R, *et al* (2014) Virchows Arch 465:599-605.
4. Hung YP *et al* (2016) Mod Path (advanced online publication)
5. Ishida M, *et al* (2013) Am J Surg Path 37:949-59.

AMR Seminar #69

Case – 19

Contributed by: Saul Suster, M.D.

(Courtesy of Dr. Trent McBride, Phoenix, AZ).

Clinical History: A 78 year old man without any significant past history was found to have bilateral lung nodules that were followed radiographically for a year. While undergoing a coronary artery bypass, a wedge biopsy of one of the lesions was performed.

Pathologic findings: The gross specimen was described as a 3.5 x 1.8 x 1.3 wedge of lung containing a well-circumscribed 2.5 x 2.0 x 1.0 cm pink-tan nodule extending from the pleura. The histology showed an endobronchial lesion with a papillary configuration. The club-like papillae were lined by a single layer of cuboidal epithelial cells and contained in their cores a monotonous population of small, round to oval cells with abundant clear cytoplasm. Scattered mitotic figures were present (averaging 2 mitoses per 10 HPF). Immunohistochemical stains showed cytoplasmic positivity of the tumor cells for S-100 protein and CD10, and negative staining for desmin, EMA, inhibin, TTF1 and melanoma cocktail. A MIB-1 stain showed ~10% nuclear positivity.

Diagnosis: Low-grade epithelioid neoplasms, NOS.

Discussion: I'm not sure what this tumor is and have never seen a similar case in the lung before. The consulting pathologist suggested a diagnosis of pulmonary hamartoma, but I have never seen a hamartoma displaying these features. In my consultation letter I offered the suggestion that this may represent an *ossifying fibromyxoid tumor* of the lung, both based on the histology and the results of the IHC (S100/CD10+). Granted that we don't know what the other lesion in the contralateral lung was (and there is always the possibility that it may be unrelated) but given the bilaterality, I suggested the possibility of an occult or unapparent soft tissue tumor that might have given rise to metastases to the lung. I have not heard from the referring pathologist yet, but wanted to obtain the opinion of the members regarding this lesion. Is it possible that this may correspond to a primary lung OFMT? If not, what could this be? Am I missing something here?

AMR Seminar #69

Case – 20

Contributed by: Ady Yosepovich, M.D.

Case History: This 51 year old lady noticed a mass in her left breast. The mammography and US were unremarkable. MRI showed asymmetry and architectural distortion in the left inner-inferior quadrant that was enhanced by gadolinium.

A MRI guided vacuum assisted biopsy was performed that was interpreted as ADH, followed by an excisional biopsy.

The slide is from the lumpectomy specimen. Since I am not sure that all slides contain the diagnostic area, I send you a few pictures as well.

The breast parenchyma shows cysts with thyroid like colloid material.

I think that this is a cystic hyper secretory lesion of the breast.

There are prominent cystic hyper secretory changes, but focally the lining cells show micro papillary proliferation.

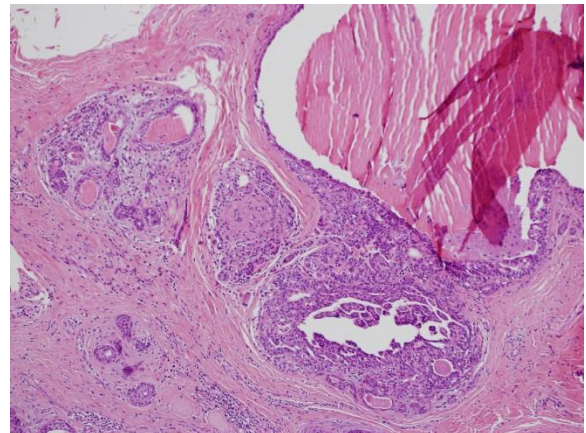
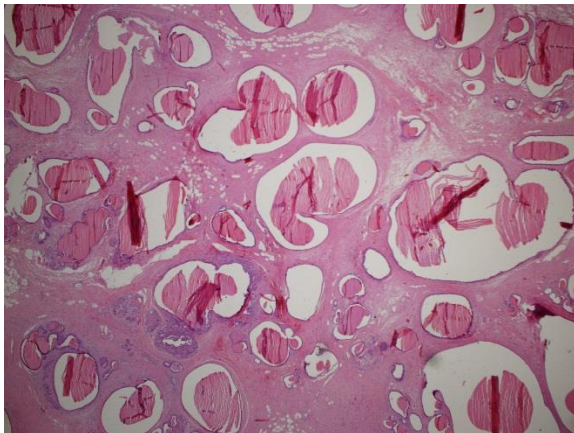
I showed those areas to my colleges in my department.

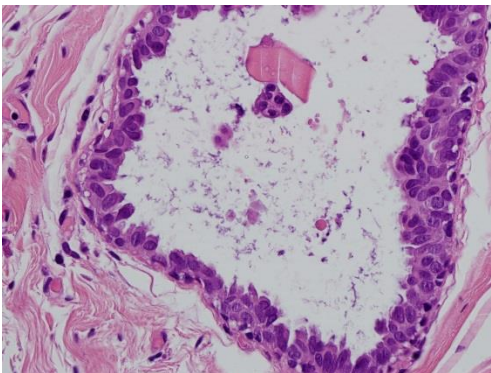
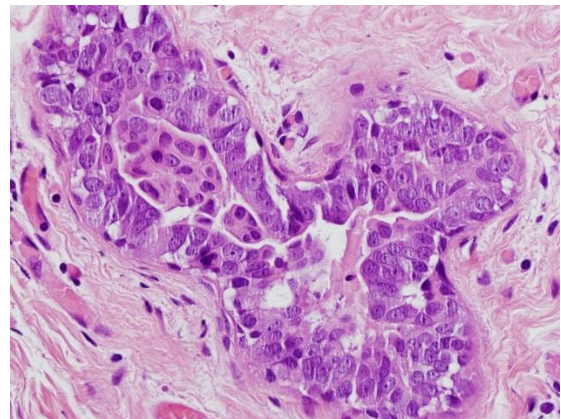
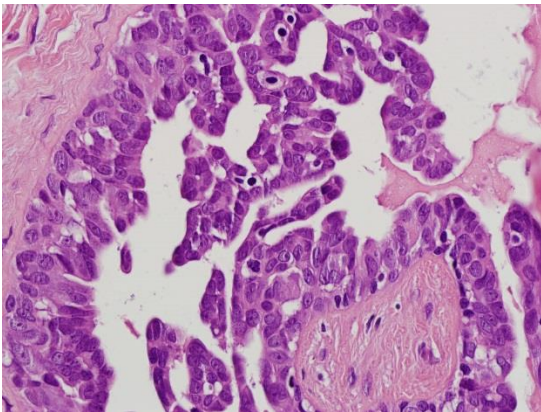
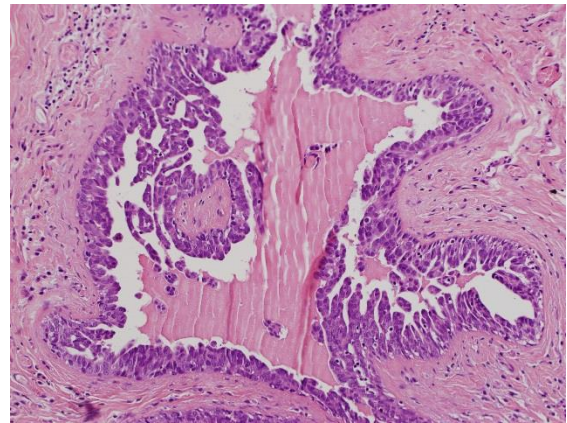
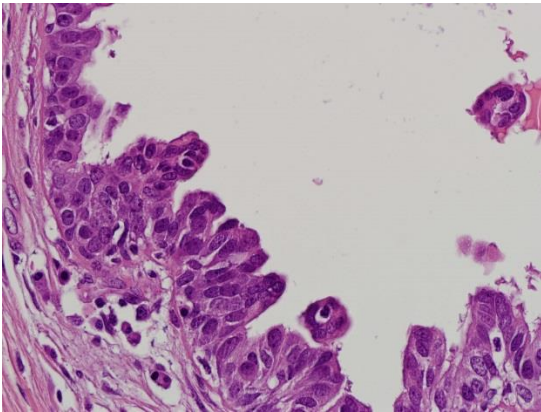
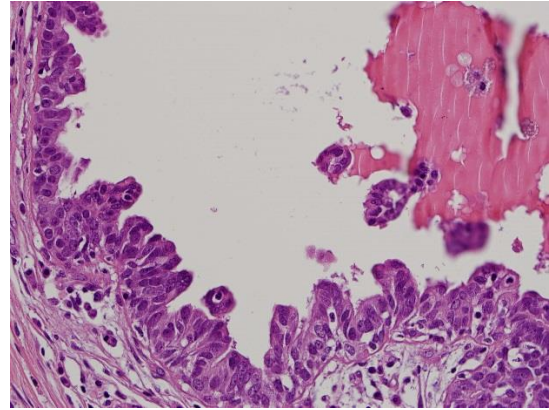
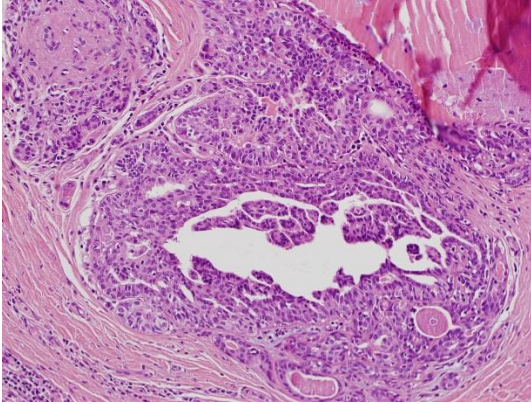
Do you think this is micro papillary DCIS?

Rosen's book has a section on these lesions that were first described in 1984 by Rosen and Scott. It appears to be an unusual lesion with no present study to evaluate its molecular and genetic alterations. I must admit that it was a tough judgment call for me – even after reading this chapter and looking at all the pictures.

Diagnosis: Finally, I concluded this as a cystic hyper secretory lesion with small areas of micro papillary DCIS –

I would very much like to have your opinions





AMR Seminar #69

Case – 21

Contributed by Ady Yosepovich, M.D.

Case History: This case was brought to unofficial consultation by Dr. Dvora Kidron, Head of the department of pathology at the Meir Medical Center, Israel, and was prepared by her.

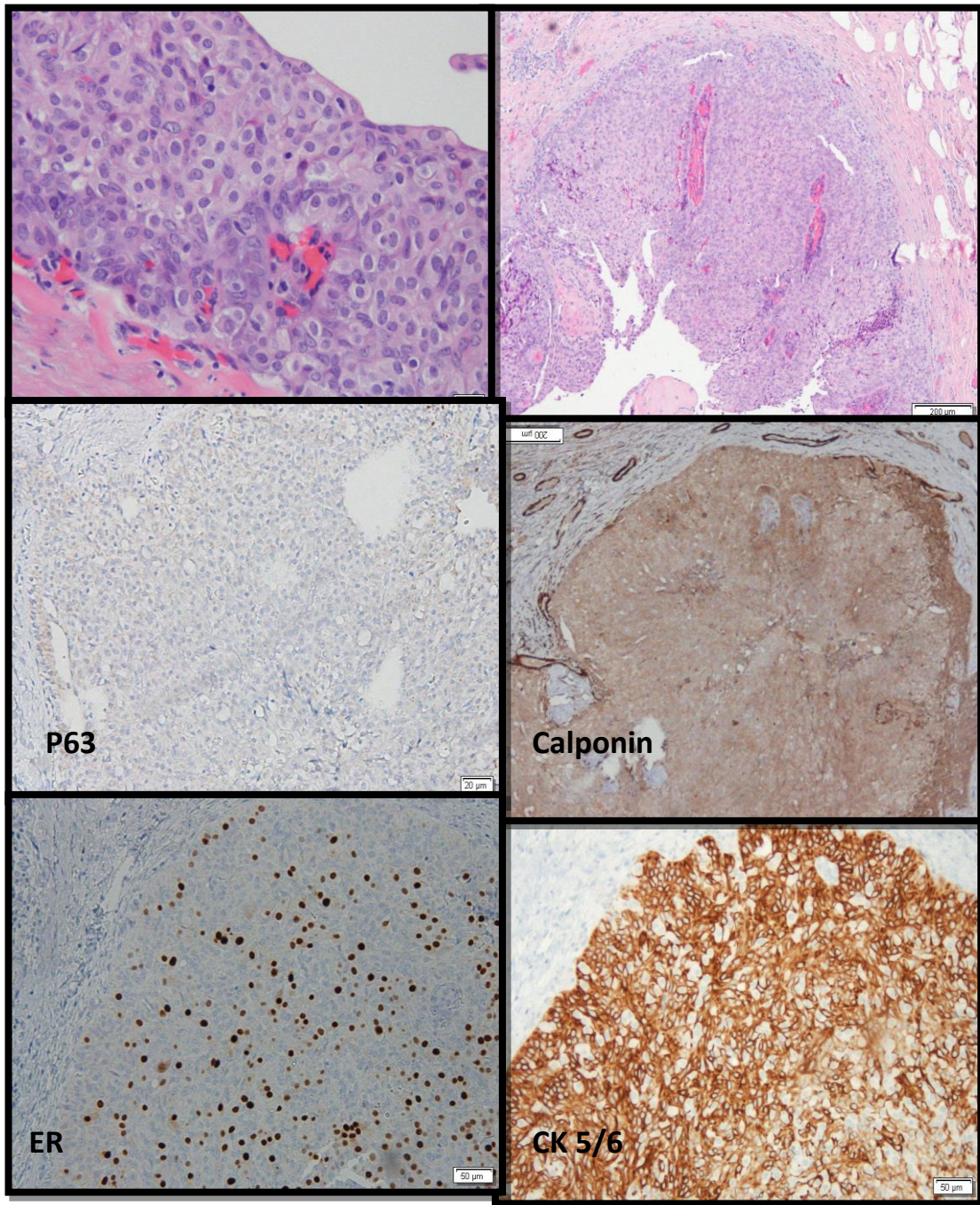
We discussed the differential diagnosis on length on several occasions, learned a lot out of the intensive brainstorming. I apologize for sending a second case this round, but I cannot resist sharing this case with you. We would very much like to get your remarks and your thoughts of what we think is an exceptional and intriguing case.

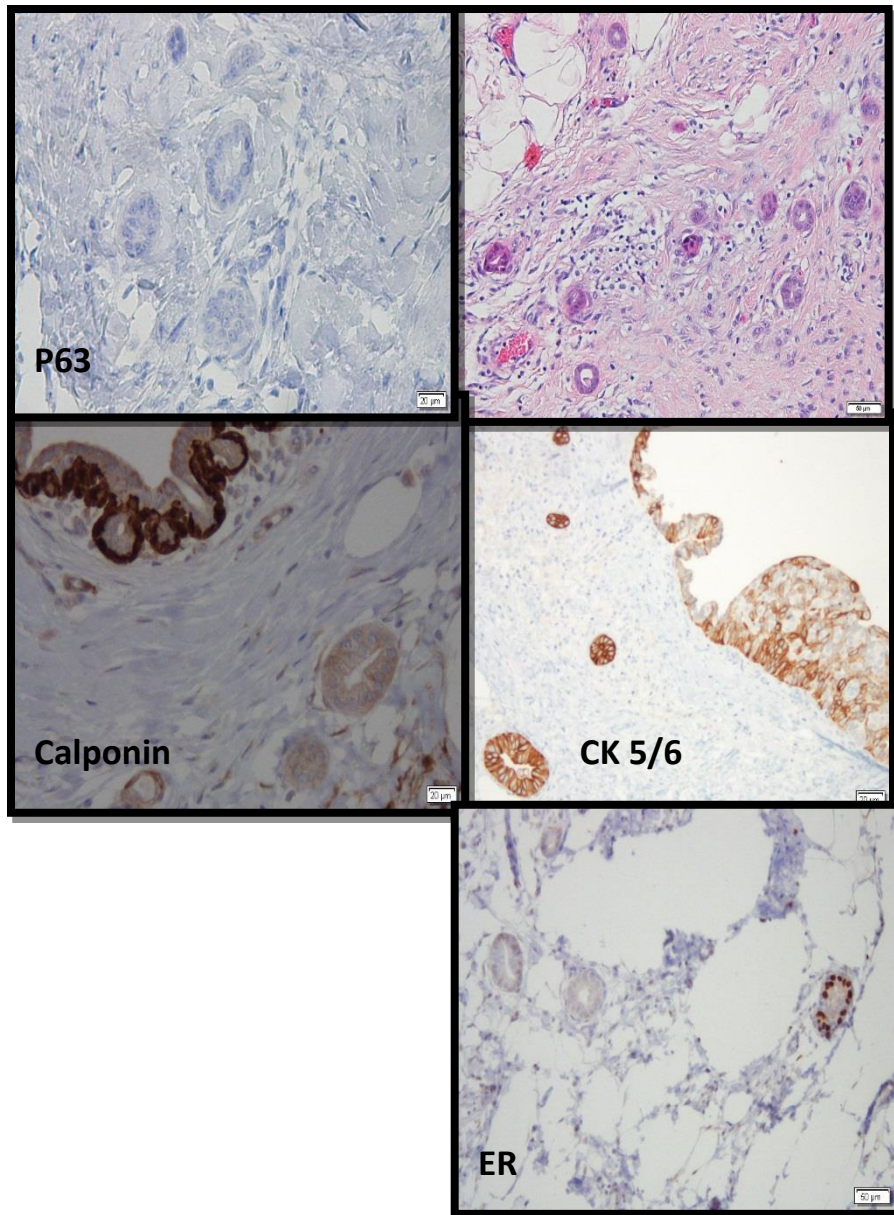
The patient is 70 years old. A hypoechoic mass, 1.2 cm in diameter, was noted on the right breast, 2 Cm away from the nipple. Intracystic papillary carcinoma was diagnosed in tru-cut biopsy. Lumpectomy was carried out 6 weeks later. Grossly, a 1cm mass was seen. It consisted of a papillary lesion and numerous small epithelial nests, usually embedded in fibrous tissue.

Results of Immunohistochemical stains:

	Intraductal lesion	Small epithelial nests
Calponin	-	-
P63	-	-
CK5/6	Mixed: + and -	Some +, some -
S100	Positive in 30%	Some +, some -
ER	Positive in 30%	Some +, some -

The papillary lesion





The epithelial nests in the stroma

The diagnostic dilemmas:

1. The nature of the intraductal lesion: intracystic carcinoma? Atypical papilloma? a papilloma with florid ductal hyperplasia?
2. The nature of the small epithelial nests: epithelial displacement (rather extensive)? IDC?
3. We are pretty convinced that the small epithelial proliferation is due to displacement post core needle biopsy of a papillary lesion.

We are debating if the papillary lesion is malignant or not. We will appreciate your opinions.

AMR Seminar #69

Quiz Case -1

Contributed by: Thomas V. Colby, M.D.

Case: A 46-year-old HIV-positive man presented with recurrent pneumothorax. Imaging studies were said to be suspicious for pneumocystis, in addition, showing features for pneumothorax.

AMR Seminar #69

Quiz Case -2

Contributed by: Saul Suster, M.D.

Clinical History: A 32 year old man was seen for a palpable nodule in his orbital region. A 2.0 x 2.0 x 1.5 cm ovoid and firm soft tissue mass was resected.